SCIEPublish

Review

Unravelling the Role of Hydrogen Evolution Reaction Co-Catalysts in Photocatalytic Water Splitting: Mechanistic Insights and Material Strategies

Bhagatram Meena, Preetha Chandrasekharan Meenu and Panagiotis G. Smirniotis *

Department of Chemical and Environmental Engineering, University of Cincinnati, Cincinnati, OH 45221-0012, USA; bhagatrammeena1010@gmail.com (B.M.); meenupc06@gmail.com (P.C.M.)

* Corresponding author. E-mail: smirnipp@ucmail.uc.edu (P.G.S.)

Received: 14 January 2025; Accepted: 18 February 2025; Available online: 7 March 2025

ABSTRACT: The reliance on fossil fuels has led to a substantial increase in greenhouse gas emissions, presenting a critical environmental challenge. Addressing this issue necessitates the adoption of alternative renewable energy sources, with green hydrogen emerging as a promising candidate due to its high gravimetric energy density and absence of harmful emissions. Among the various hydrogen production techniques, photocatalytic technology has garnered significant attention for its dual potential to produce green hydrogen and degrade pollutants, thereby addressing both energy and climate crises. Efforts to scale photocatalytic technology for industrial applications have identified cocatalyst integration as a pivotal strategy, as it enhances reaction kinetics by lowering the activation energy and mitigating charge carrier recombination. This review comprehensively examines the hydrogen economy, the underlying principles of photocatalysis, recent technological advancements, key factors influencing photocatalytic reactions, the role of catalysts in hydrogen evolution reaction (HER) surface mechanisms, strategies for cocatalyst optimization, and future directions for the field.

Keywords: Photocatalysis; HER; CO-catalyst; Surface reactions; Charge recombination

1. Introduction

1.1. Background of Photocatalytic Water Splitting

With the growing global population and rapid advancements in technology, the demand for energy is rising concurrently, leading to an increased reliance on fossil fuels such as coal, oil, and natural gas [1,2]. This escalating consumption of fossil fuels has become a major contributor to climate change, posing a significant global concern [3–5]. The energy sector remains the largest source of CO_2 emissions, with electricity generation and transportation playing pivotal roles due to their heavy dependence on fossil fuels [6–8]. In 2008, the global energy consumption rate was 15 TW, and it is projected to rise to 19.5 TW for primary energy and approximately 3 TW for electricity alone [9–11]. Hydrogen offers a viable alternative to fossil fuels because of its high gravimetric energy density and the absence of harmful byproducts [12,13]. Various methods exist for hydrogen production, including electrocatalysis, photoelectrochemical water splitting, thermochemical water splitting, and photocatalysis [14–24]. Among these, photocatalysis has garnered significant attention due to its ability to harness renewable resources such as sunlight and water, in conjunction with semiconductor materials, to produce hydrogen without requiring external bias and at a low cost [25,26]. In 1972, Fujishima and Honda achieved a groundbreaking milestone in hydrogen production by demonstrating water splitting using a TiO_2 semiconductor as a photoactive material under UV light, leading to hydrogen (H_2) generation [27]. The photocatalytic water splitting process involves the following key steps: (i) Solar Light Absorption: Semiconductor materials absorb solar light, generating excitons (electron-hole pairs) or charge carriers. (ii) Charge Carrier Transportation: The generated charge carriers are transported to the surface of the semiconductor. (iii) Surface Reactions: At the photocatalyst surface, oxidation and reduction reactions occur, resulting in the production of

https://doi.org/10.70322/prp.2025.10005

O_2 and H_2, respectively, as illustrated in Figure 1 [28,29]. The efficiency of hydrogen production via photocatalysis is influenced by several factors, including solar harvesting ability: Efficient absorption of solar radiation by the semiconductor. Semiconductor Stability: Stability of the semiconductor material in aqueous media during the reaction. Charge Separation: Effective separation of charge carriers to prevent recombination. Low Charge Recombination: Minimizing the recombination of electrons and holes to enhance the overall reaction efficiency. These factors collectively determine the feasibility and scalability of photocatalytic hydrogen production [30–32].

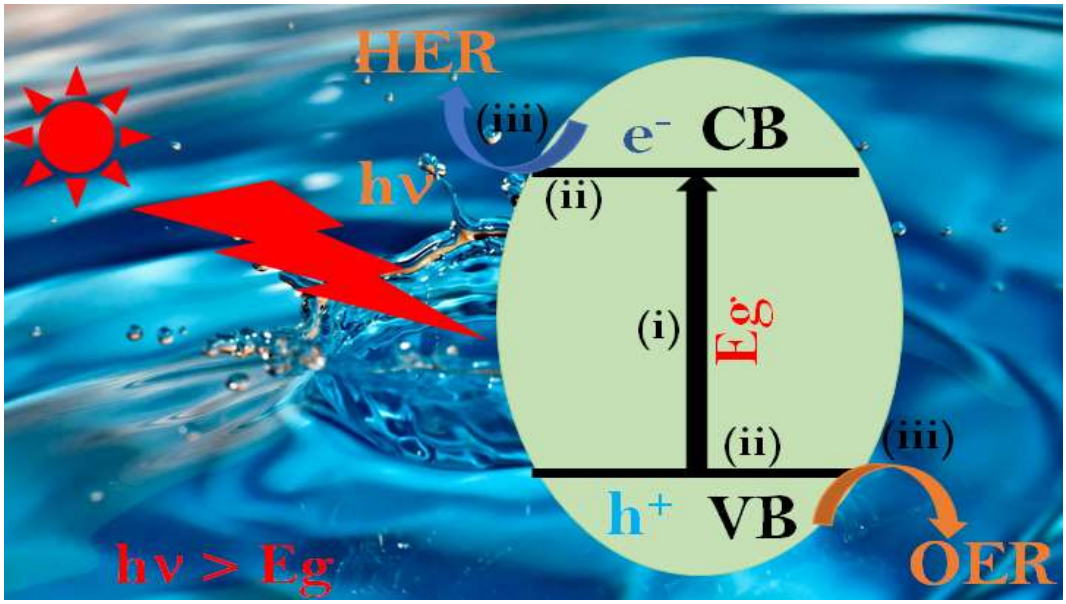

Figure 1. Basic representation of photocatalysis for water splitting.

1.2. Evaluating Efficiency in PCWS

Efficiency of the PCWS can be decided by two measure factors: One is Turnover Frequency (TOF) and the other is Apparent Quantum Efficiency (AQE). Here we will discuss them in detail.

1.2.1. Turnover Frequency (TOF)

Turnover Frequency (TOF) is a widely used parameter for evaluating the efficiency of photocatalysts in photocatalytic water splitting. TOF quantifies the number of product molecules (H_2 or O_2) generated per active site of the photocatalyst per unit time, providing a measure of the intrinsic catalytic activity. Unlike overall yield, TOF is independent of the amount of catalyst used, making it a more reliable indicator of the photocatalyst's performance. TOF can be calculated by below mentioned equations.

$$\text{TOF}\ (S^{-1}) = \frac{\text{NO. of Products}}{\text{No. of active sites} \times \text{Reaction time}}$$

$$\text{TOF}\ (S^{-1}) = \frac{\text{NO. of reacted electrons}}{\text{No. of atoms in the photocatalyst}}$$

$$\text{TOF}\ (S^{-1}) = \frac{\text{NO. of reacted electrons}}{\text{No. of atoms on the surfaces or specific surface area}}$$

In summary, a higher TOF directly correlates with superior photocatalytic performance, showcasing the photocatalyst's ability to efficiently convert absorbed energy into chemical products [33].

1.2.2. Apparent Quantum Efficiency

AQE is also another critical parameter to evaluate the efficiency of the photocatalyst in the PCWS. AQE represents the capacity of a photocatalyst to convert incident photons into chemical energy during the PCWS process. It provides critical insights on the photocatalyst's ability to utilize sunlight, making it an important parameter in PCWS technology. AQE can be measured by the below mentioned equation [34].

$$\text{AQE (\%)} = \frac{\text{No. of electrons utilized in product formation} \times 100}{\text{No. of Incident Photons}}$$

No. of electrons for H_2 and O_2 are 2 and 4, respectively. The AQE can be expressed in another way as well.

$$\text{AQE (\%)} = \frac{\text{No. of } H_2 \text{ or } O_2 \times \text{electrons per molecule} \times \text{Avogadro number} \times 100}{\text{Incident photon flux} \times \text{Area} \times \text{time}}$$

1.3. Strategies to Enhance the Efficiency of Photocatalyst

To enhance photocatalytic efficiency, numerous strategies have been developed to broaden solar energy absorption and improve charge separation and migration. Key approaches include heterojunction formation, metal/non-metal doping, morphology engineering, surface plasmon resonance (SPR) metal particle loading, and cocatalyst loading, as illustrated in Figure 2.

(i). Heterojunction Formation: This strategy combines two materials with different band gaps to extend the photocatalyst's absorption into the visible light region. The heterojunction structure facilitates better charge separation and generates a higher density of charge carriers, improving the photocatalytic process [35,36]. Various types of heterojunction systems exist, including type-II, S-scheme, Z-scheme, p-n junction, and J-type heterojunctions [37]. Among these, J-type heterojunctions have recently attracted significant attention due to their remarkable anisotropic electrical properties. When the energy band alignment of a J-type heterojunction resembles that of a type-II heterojunction, where only the first semiconductor is exposed to light, photoexcited electrons migrate from the CB of the first semiconductor to the CB of the second semiconductor, while the photoinduced holes remain in the VB of the first semiconductor. This spatial separation of charge carriers enhances hydrogen evolution efficiency. However, constructing J-type heterojunctions presents a significant challenge, particularly due to the anisotropic electrical conductivity of materials such as $ZnIn_2S_4$. The design of these heterojunctions must not only optimize photoinduced charge separation but also ensure efficient charge transport. Anisotropic electrical conductivity refers to the directional dependence of electrical transport properties within a material. This anisotropy can arise due to variations in crystal structure, intrinsic defects, or electronic band configuration, all of which influence charge carrier dynamics [38–41].

(ii). Metal/Non-Metal Doping: Substituting guest metal or non-metal elements into pristine materials modifies their electronic band structure. This adjustment makes the photocatalyst more active under visible light, increases charge carrier density, and enhances the oxygen evolution reaction (OER) and hydrogen evolution reaction (HER) at the photocatalyst interface [42,43].

(iii). Morphology Engineering: By employing capping agents and varying reaction conditions, the photocatalyst's morphology can be optimized. These modifications influence the material's electronic and structural properties, increasing the number of active sites for OER and HER at the interface [44–46].

(iv). Surface Plasmon Resonance (SPR): Loading SPR-active metal particles (e.g., Au, Ag) on the photocatalyst enhances absorption in the visible light region. When the irradiated light matches the resonance energy of these metals, their conduction band electrons are excited, boosting charge carrier density and facilitating photocatalytic water splitting [47].

(v). Cocatalyst Loading: Cocatalyst loading involves integrating electroactive materials onto the photocatalyst surface to enhance photocatalytic efficiency. Cocatalysts facilitate efficient charge transfer by capturing charge carriers promptly, thereby improving charge separation. This process significantly reduces the activation energy required for water splitting, accelerating reaction kinetics [48,49]. Additionally, cocatalyst loading enhances the stability of the photocatalyst by minimizing direct contact between the semiconductor and the aqueous media, thereby preventing degradation. These properties make cocatalyst strategies highly appealing for practical applications. Key benefits of cocatalyst loading include reduction in threshold potential and lowering the energy barrier for reactions, enabling easier hydrogen production and pollutant degradation. The presence of cocatalysts speeds up surface reactions by efficiently mediating charge transfer. Improved Photocatalyst Stability: By shielding the photocatalyst from direct interaction with aqueous environments, cocatalysts enhance the long-term operational stability. Due to these distinctive properties, cocatalyst strategies are considered highly effective for long-term hydrogen production and pollutant degradation. These advancements could play a crucial role in addressing energy crises and mitigating climate change by supporting sustainable and efficient photocatalytic systems [28,50,51].

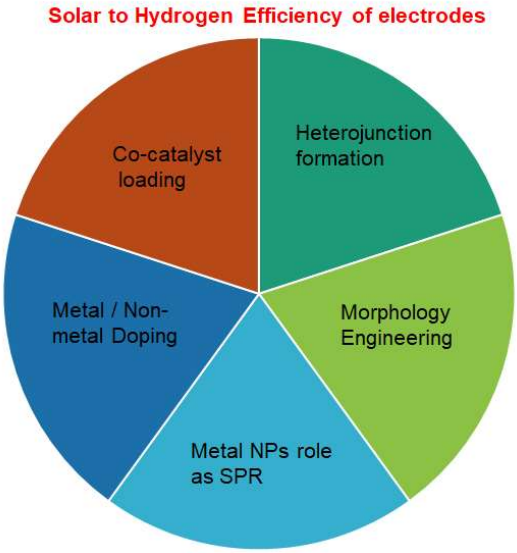

Figure 2. Strategies to Improve the Efficiency for the photocatalyst/Photoelectrodes.

Cocatalysts play a crucial role in enhancing the efficiency of photocatalytic water splitting by selectively optimizing the respective half-reactions. They are classified into two main types: oxygen evolution cocatalysts (OECOs) and hydrogen evolution cocatalysts (HECOs) [52–55]. OECOs enhance the oxygen evolution reaction (OER) by increasing the reaction rate and reducing the activation energy. They are further categorized into noble metal-based, non-noble metal-based, and metal-free cocatalysts, with noble metal oxides such as RuO_2 and IrO_2 being widely studied for their superior OER activity. These cocatalysts significantly improve overall water-splitting efficiency by facilitating oxygen release [56,57]. Conversely, HECOs enhance the hydrogen evolution reaction (HER) by accelerating the reaction rate, reducing activation energy, and mitigating charge recombination through efficient electron acceptance, thereby increasing hydrogen production. HECOs are classified into noble metal-based, non-noble metal-based, and metal-free cocatalysts. Among them, noble metals such as Pt, Ru, Rh, Pd, Au, and Ag have been widely studied [58–63]. Pt stands out as the most efficient HECO due to its high work function, excellent conductivity, and lowest overpotential for HER. Photocatalysts loaded with Pt have demonstrated the highest photocatalytic efficiency for hydrogen production under sunlight [64]. Achieving efficient overall water splitting requires: Minimizing backward reactions: Suppressing the recombination of hydrogen and oxygen gases, as well as preventing photoreduction of oxygen. Selective Cocatalyst Activity: Cocatalysts must be highly active and selective to promote forward HER and OER reactions while inhibiting side reactions. Among state-of-the-art cocatalysts, $Rh_{2-y}Cr_yO_3$ and core–shell-structured Rh-Cr_2O_3 have shown remarkable performance in facilitating HER [65,66]. These materials effectively suppress backward reactions, enhance charge separation, and improve overall water-splitting efficiency. This combination of OECOs and HECOs, along with high-activity and selectivity cocatalysts, forms the backbone of advanced photocatalytic systems, making them highly promising for sustainable hydrogen production and addressing energy challenges. The noble-metal-based cocatalysts mentioned earlier, while highly efficient, face limitations due to their high cost and scarcity, rendering them unsuitable for large-scale energy applications. Consequently, there is a growing emphasis on developing cost-effective and efficient cocatalysts derived from abundant and inexpensive materials.

Recent research has introduced innovative cocatalysts based on non-noble metals based have shown promise in enhancing photocatalytic water-splitting performance. Additionally, materials like MoS_2 and graphene have gained attention due to their synergistic effects. For instance, studies have demonstrated a significant improvement in photocatalytic efficiency when graphene and MoS_2 are used as cocatalysts with TiO_2-based photocatalysts. This synergy enhances charge separation, electron mobility, and active site availability, leading to better HER efficiency [67,68]. Given the significant advancements in the field of photocatalytic water splitting, particularly in the development of HECOs, there is a need for a comprehensive review to consolidate recent findings. This review will focus on their role in HER reactions, understanding how cocatalysts facilitate HER and influence the reaction pathway, exploring factors like charge separation, surface area, and stability, and highlighting breakthroughs in affordable, non-noble metal cocatalysts such as transition metal hydroxides, sulfides, and carbon-based materials. This review aims to provide a detailed understanding of the current state of research in HECOs, serving as a foundation for future advancements in the development of sustainable and scalable photocatalytic systems for hydrogen production.

2. Requirement of Cocatalyst Loading in Photocatalytic Water Splitting (PCWS)

2.1. Role of Cocatalyst Loading in PCWS

Photocatalytic water splitting has emerged as a promising alternative to conventional energy production pathways, offering the potential to reduce reliance on fossil fuels and mitigate climate change. This technology enables the production of green hydrogen as a clean, sustainable fuel using abundant renewable resources such as sunlight and water. By harnessing these resources, photocatalytic water splitting addresses the growing energy demand while contributing to climate change mitigation, a critical concern for current and future generations. The performance of photocatalytic systems is influenced by several factors, including semiconductor band edge positions, charge carrier generation rates, charge transportation, photocorrosion in aqueous media, and high charge recombination rates of electrons and holes, which reduce the availability of charge carriers for surface reactions. To address these challenges, cocatalyst technology has garnered significant attention. Cocatalysts enhance photocatalytic efficiency by lowering the energy barrier for water splitting reactions, capturing photogenerated holes or electrons, thereby suppressing charge recombination and protecting the photocatalyst from photocorrosion in aqueous environments. By integrating cocatalysts, the reaction rates are accelerated, and the durability of the photocatalyst is significantly improved, making photocatalytic water splitting a viable solution for sustainable hydrogen production and a key technology in addressing global climate challenges.

2.2. Key Factors for Affecting Cocatalyst Performance in PCWS

As discussed in Section 2.1, the incorporation of cocatalysts offers significant advantages in enhancing PCWS performance, particularly for the HER and overall water splitting. However, the efficiency of this process is influenced by several critical factors, as illustrated in Figure 3. The most common forms of cocatalysts are transition metal oxides or oxyhydroxides, sulfides (NiS_2, CoS), phosphides (CoP, Ni_3P_2), and noble metals (Pt, Pd, Ru, Rh, and Ir). Performance is significantly impacted by the type of cocatalyst [67,69]. Noble metal-based cocatalysts, with their small overpotential and easy electron transfer tendency, have demonstrated improved catalytic activity for HER. However, inexpensive, non-noble metal-based materials are gaining popularity because they are easy to prepare and have ideal size and dimensions, which speed up the rate of reaction by supplying more active sites. Here we will discuss the reaction affecting factor with the cocatalyst loading.

(i). Electronic and band alignment properties: The electronic properties, particularly the work function of a cocatalyst, play a critical role in determining the efficiency of PCWS. As an electroactive material, the cocatalyst accelerates reaction rates by facilitating charge transfer and reducing charge recombination, but its effectiveness depends heavily on the band alignment with the photocatalyst. The alignment of energy levels between the photocatalyst and cocatalyst is crucial for enabling efficient charge transfer, directly impacting the product efficiency and reaction mechanism. The conduction band (CB) of the photocatalyst must be more negative than the hydrogen evolution potential (0 V *vs.* SHE). The cocatalyst must efficiently capture and transfer the photogenerated electrons from the CB of the photocatalyst to drive HER. The synergy between the photocatalyst and cocatalyst, driven by proper band alignment and electronic properties, is vital for optimizing PCWS. In HER systems, a conduction band more negative than 0 V and a cocatalyst capable of timely electron capture and transfer are essential for achieving high efficiency. By tailoring these electronic interactions, it is possible to enhance the overall performance and scalability of photocatalytic systems [69].

(ii). The interfacial interaction between the photocatalyst and the cocatalyst is a critical factor that facilitates effective charge separation and suppresses charge recombination in PCWS. A strong interaction ensures efficient transfer of photogenerated electrons or holes from the photocatalyst to the cocatalyst, enhancing the reaction rate and overall efficiency. Optimizing synthesis procedures and minimizing interface defects are essential for ensuring effective charge separation, suppressing recombination, and maximizing photocatalytic performance [48].

(iii). Catalytic selectivity is a critical factor in the PCWS technology, as it determines the preferential enhancement of desired reactions while suppressing unwanted side reactions. For efficient PCWS, the cocatalyst must exhibit high selectivity to ensure the effective generation of H_2 and O_2 while minimizing competing processes, such as H_2O_2 formation or backward reactions. This ensures higher yields of H_2 and O_2, improved catalyst durability, and more efficient use of solar energy [70].

(iv). Both the loading amount of cocatalysts and the reaction atmosphere are crucial factors influencing the efficiency and durability of photocatalytic water splitting (PCWS). These parameters must be carefully optimized to achieve

the desired reaction performance and long-term stability of the photocatalyst. The amount of cocatalyst loaded onto the photocatalyst significantly impacts the overall efficiency of PCWS by optimal loading, underloading, and overloading. As underloading may fail to provide required active sites on the cocatalyst surface whereas overloading could block the semiconductor surface from being exposed to sunlight, which results in the generation of a smaller amount of charge carriers, it may also lead to the agglomeration of cocatalyst particles on the semiconductor surface which could again inhibit the active sites and impact the PCWS activity. The reaction atmosphere, including pH**,** temperature, and surrounding gas conditions, plays a critical role in PCWS performance. Considering factors like pH, temperature, and the surrounding gas environment, alongside precise cocatalyst loading, can significantly improve the overall performance and long-term stability of photocatalytic systems [71].

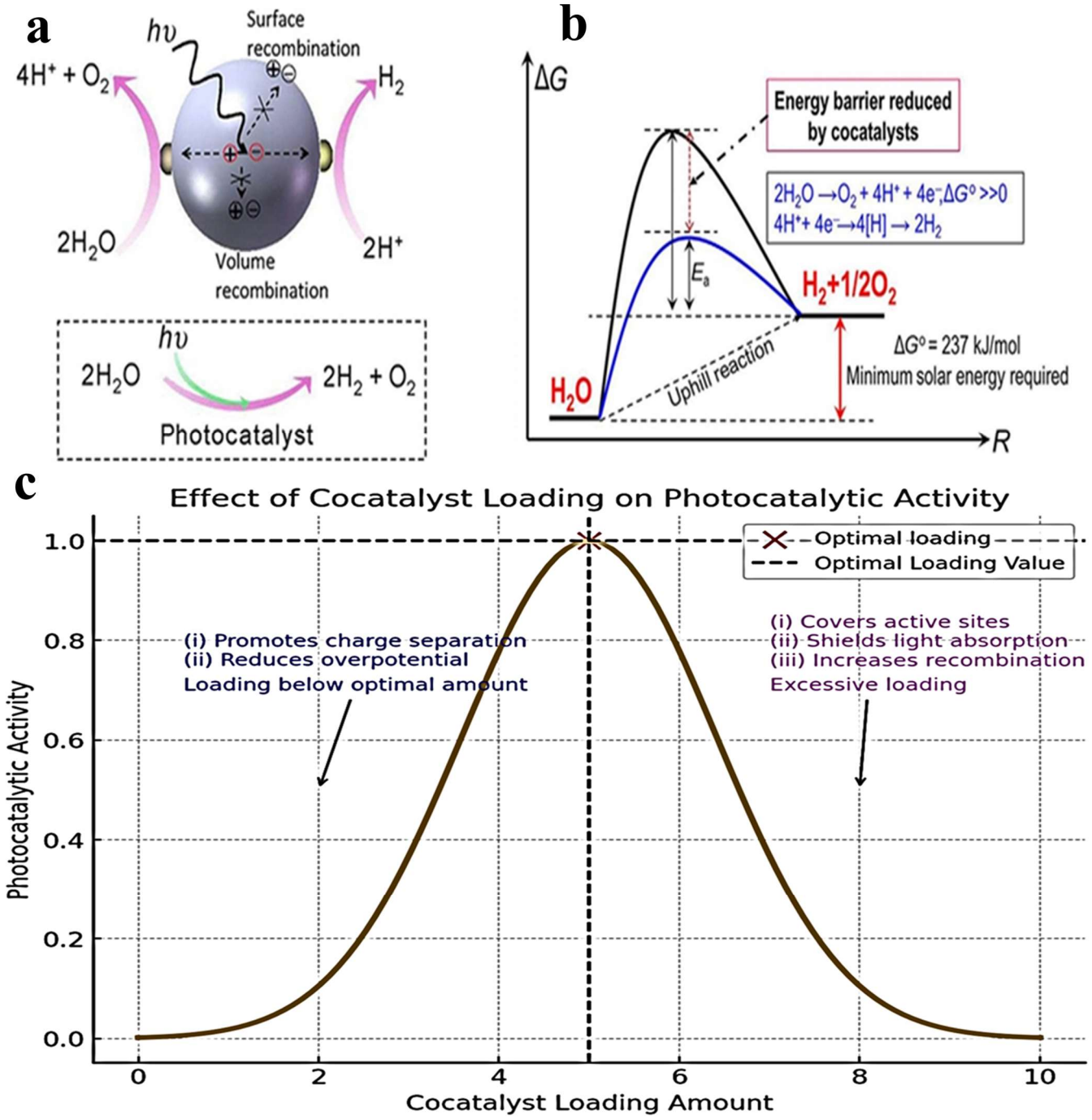

Figure 3. (**a**,**b**) Schematic shows the function and the intrinsic role of the semiconductor in reducing the activation barrier in overall water splitting. Reproduced with permission from Ref [48]. Copyright © 2013, American Chemical Society. (**c**) A volcano-type relationship between the loading amount of a cocatalyst and the photocatalytic activity of the cocatalyst-loaded semiconductor photocatalyst. Inspired from Ref [69].

3. Classifications of HER Cocatalyst in PCWS

HER-based cocatalysts are essential components in PCWS, where they play a pivotal role in facilitating the reduction of protons to molecular hydrogen (H_2). These cocatalysts are classified into distinct categories based on their compositional and functional characteristics, each offering specific advantages and facing certain limitations. This section delves into these classifications, providing a detailed exploration of their properties and discussing recent advancements that contribute to a deeper understanding of their roles in PCWS.

3.1. Noble Metal Based Cocatalyst

Cocatalysts have proven to be a highly effective strategy for mitigating charge recombination in PCWS, thereby enhancing the efficiency of the HER. Among these, noble metals have exhibited outstanding catalytic performance for HER, attributed to their advantageous electronic properties, such as low overpotential and optimal work function values, which facilitate efficient charge transfer and favorable reaction kinetics. This section examines the most extensively studied noble metal-based cocatalysts, specifically platinum (Pt), palladium (Pd), and rhodium (Rh), highlighting their roles and recent advancements in the field.

3.1.1. Pt Based Cocatalyst for HER

Platinum (Pt) has long been regarded as the benchmark cocatalyst for the HER in PCWS due to its near-zero hydrogen adsorption free energy (ΔG_{H^*}). This property facilitates efficient proton adsorption and desorption, which are critical steps in HER. When loaded onto the surface of a photocatalyst, Pt acts as an electron collector, accelerating the reaction rate and suppressing charge recombination. These characteristics have made Pt a subject of extensive exploration in PCWS. Recently, Li et al. reported the Tb_4O_7/CN heterojunction photocatalyst loaded with Pt cocatalysts using two distinct Pt precursors with opposite charges: $[PtCl_6]^{-2}$ (negatively charged) and $[Pt(NH_3)_4]^{+2}$ (positively charged). The negative precursor led to selective Pt loading on the positive Tb_4O_7 section of the heterojunction, forming Pt@Tb_4O_7/CN. This synergistic configuration enhanced charge separation between Tb_4O_7 and CN, facilitating efficient electron transfer. This approach led to higher H_2 Evolution Rate of 132 $\mu molh^{-1}g^{-1}$, a significant improvement due to the strong interaction between Pt, Tb_4O_7, and CN. When the positive precursor resulted in Pt loading on the negative CN section, forming Tb_4O_7/CN@Pt. This configuration was anti-synergistic, as it disrupted the charge separation and reduced the interaction between photocatalyst components. This approach led them to lower the H_2 evolution rate to 18.2 $\mu molh^{-1}g^{-1}$, lower than both Pt@ Tb_4O_7/CN and even the bare Tb_4O_7/CN heterojunction. As shown in Figure 4a, the synergistic configuration demonstrates the facile charge transfer across the heterojunction where photogenerated electrons are efficiently collected by Pt on Tb_4O_7. The alignment of the band edges ensures effective separation of charge carriers, leading to enhanced H_2 production. In this case, an anti-synergistic configuration displays a mismatch in band edge alignment, hindering charge transfer and resulting in poor hydrogen production efficiency. This study highlights the critical role of precursor selection and site-specific Pt loading in achieving optimal interaction between the photocatalyst and cocatalyst. The Pt@Tb_4O_7/CN heterojunction, with its synergistic charge separation, significantly enhances H_2 production efficiency, emphasizing the importance of band alignment and interfacial interactions for optimizing PCWS systems. The loading of Pt cocatalyst has been phenomenal to accelerate the reaction rate and produces good amounts of H_2 [72].

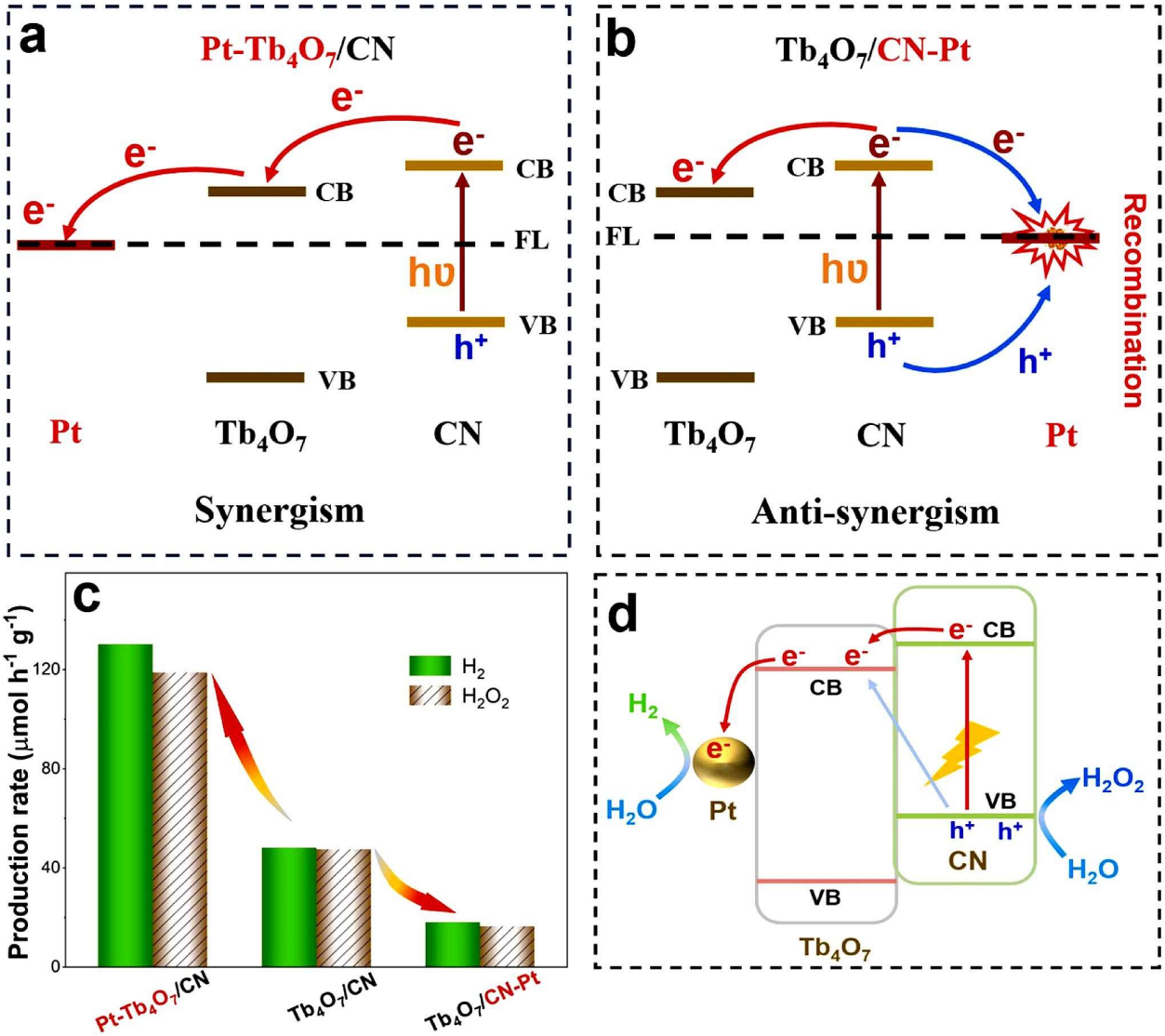

Figure 4. (**a**) Synergism charge transfer mechanism (**b**) Anti-Synergism charge transfer mechanism (**c**) Hydrogen production efficiency (**d**) Overall water splitting reaction mechanism [72].

3.1.2. Pd Based Cocatalyst for HER

Palladium (Pd), a noble metal-based cocatalyst, has shown significant potential for improving the efficiency of the hydrogen evolution reaction (HER). While not as efficient as platinum (Pt), Pd is considered a highly attractive option due to its cost-effectiveness, high work function value (greater than the water reduction potential), and tunable properties, making it a promising alternative for enhancing photocatalytic efficiency. Pd cocatalysts are typically loaded onto photocatalyst surfaces to enhance their performance. Acting as an electron sink, Pd captures photogenerated electrons from the photocatalyst and transfers them to the surface, where they reduce protons (H^+) to produce hydrogen (H_2), thus driving the HER efficiently. By timely capturing electrons, Pd forms an electron cloud at the catalyst surface, enhancing photocatalytic activity, suppressing charge recombination, and improving charge separation. Furthermore, Pd can influence both the Volmer and Heyrovsky/Tafel reaction pathways in HER, contributing to efficient hydrogen production. Inspired by these advantages, Pd has been employed with various semiconducting photocatalysts to enhance H_2 production. Recently, Zhu et al. reported a synergistic effect of Pd nanoparticles with carbon quantum dots (CQDs) for improving the HER efficiency of TiO_2 nanosheets (NSs)-based photocatalysts. In this study, the selection of this combination was selected because TiO_2 was chosen for its high photoactivity, CQDs were selected for their excellent conductivity and Pd served as a cocatalyst, acting as an electron sink to boost charge separation and suppress recombination. This composite material achieved an impressive hydrogen production rate of 13.4 mmol $h^{-1}gcat^{-1}$, which was 901.5 times higher than bare TiO_2, 41.8 times higher than 0.5CQDs/TiO_2, 1.7 times higher than Pd/ TiO_2. The enhancement in efficiency can be attributed to the proposed charge transfer mechanism, which is depicted in Figure 5a

[73]. The synergistic interaction between Pd, CQDs, and TiO_2 resulted in efficient charge separation, reduced recombination, and a significant boost in hydrogen production.

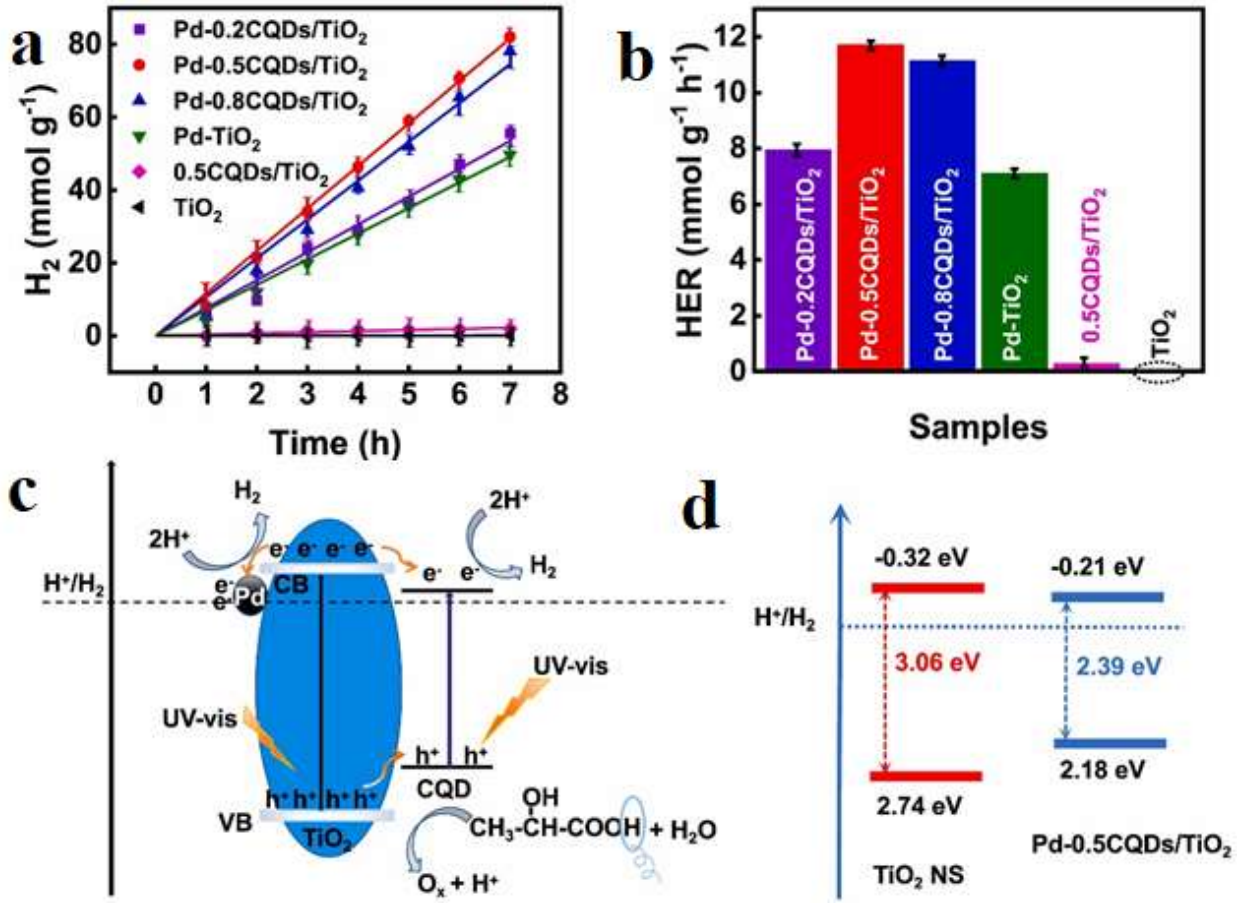

Figure 5. (**a**,**b**) Photocatalytic performances of the series of TiO_2-based samples in the lactic acid-water mixture at 25 °C. (**c**) Schematic illustration of the photocatalytic H_2 evolution mechanism over the Pd-0.5CQDs/TiO_2 catalyst in lactic acid-water mixture (**d**) Schematic illustration of the photocatalytic H_2 evolution mechanism over the Pd-0.5CQDs/TiO_2 catalyst in lactic acid-water mixture [73].

3.1.3. Rh Based Cocatalyst for HER

Rhodium (Rh), a noble metal-based cocatalyst, has garnered significant attention due to its exceptional catalytic activity for the hydrogen evolution reaction (HER). Its low overpotential for HER makes it an efficient choice for boosting photocatalytic performance. Rh exhibits excellent electrical conductivity, enabling effective charge transfer between the photocatalyst, cocatalyst, and water molecules. This efficient charge transfer reduces charge recombination, thereby enhancing HER efficiency. Additionally, Rh demonstrates high resistance to photocorrosion in aqueous environments, ensuring its durability and making it a suitable cocatalyst for practical applications.

When Rh is loaded onto a photocatalyst, it acts as an electron sink, facilitating enhanced charge separation and boosting photocatalytic efficiency. Rh can also work synergistically with metal nanoparticles, further improving the performance of the photocatalyst. Its ability to be synthesized with various morphologies through nanostructure engineering allows for increased active sites, while particle size tuning offers researchers new opportunities to optimize HER efficiency. Owing to these dynamic properties, Domen et al**.** recently reported the synergistic effect of Bi and Rh metal nanoparticles as cocatalysts on a photocatalyst $SrTiO_3$ (STO), significantly enhancing HER efficiency. The BiRh@STO composite material was prepared using a solid STO-molten (Bi_2O_3 and Rh_2O_3) reaction, where STO served as the template. Bi_2O_3 and Rh_2O_3 were used as dopant precursors. The enhancement in the photocatalytic response was attributed to a well-engineered electronic structure, characterized by the effective stabilization of the Rh^{3+} energy state, the removal of the Rh^{4+} energy state and the absence of additional defect states. These structural and electronic properties contributed to STO:Bi,Rh being the most active Rh-doped-based STO material for H_2 evolution, surpassing the activities of STO:Rh and STO:La,Rh by factors of approximately 16 and 4, respectively. The synergistic interaction between Bi and Rh in the BiRh@STO composite, coupled with the optimized electronic structure and extended visible

light activity, significantly enhanced HER efficiency. The improved charge transfer and hydrogen evolution mechanisms are depicted in Figure 6a,b, illustrating the key role of Rh and Bi as cocatalysts in this system. This study highlights the potential of Rh-based cocatalysts for advancing photocatalytic water splitting technologies [74].

In another study, Hirayama et al. demonstrated the effectiveness of Rh-Cr_2O_3 cocatalyst selectively loaded onto a $SrTiO_3$ (STO) photocatalyst, achieving excellent long-term H_2 evolution performance. The high hydrogen production efficiency was attributed to the facet-selective loading method, where the cocatalyst was strategically deposited on the active facets of the photocatalyst. The study utilized 1.2 nm $Rh_{2-x}Cr_xO_3$ nanocluster (NC) cocatalysts loaded onto 18-faceted STO (18-STO). This selective placement significantly enhanced the efficiency of H_2 production by ensuring optimized charge separation and reaction kinetics at the active sites. The photocatalyst obtained using this developed F-NCD method achieved the highest AQY to date for an STO prepared by hydrothermal synthesis. By optimizing the placement of $Rh_{2-x}Cr_xO_3$ nanoclusters on STO, the researchers achieved remarkable H_2 evolution efficiency and long-term stability. The mechanisms underlying the enhanced hydrogen production and charge transfer processes are depicted in Figure 7a,b, providing valuable insights into the role of facet-selective strategies in photocatalytic water splitting [75].

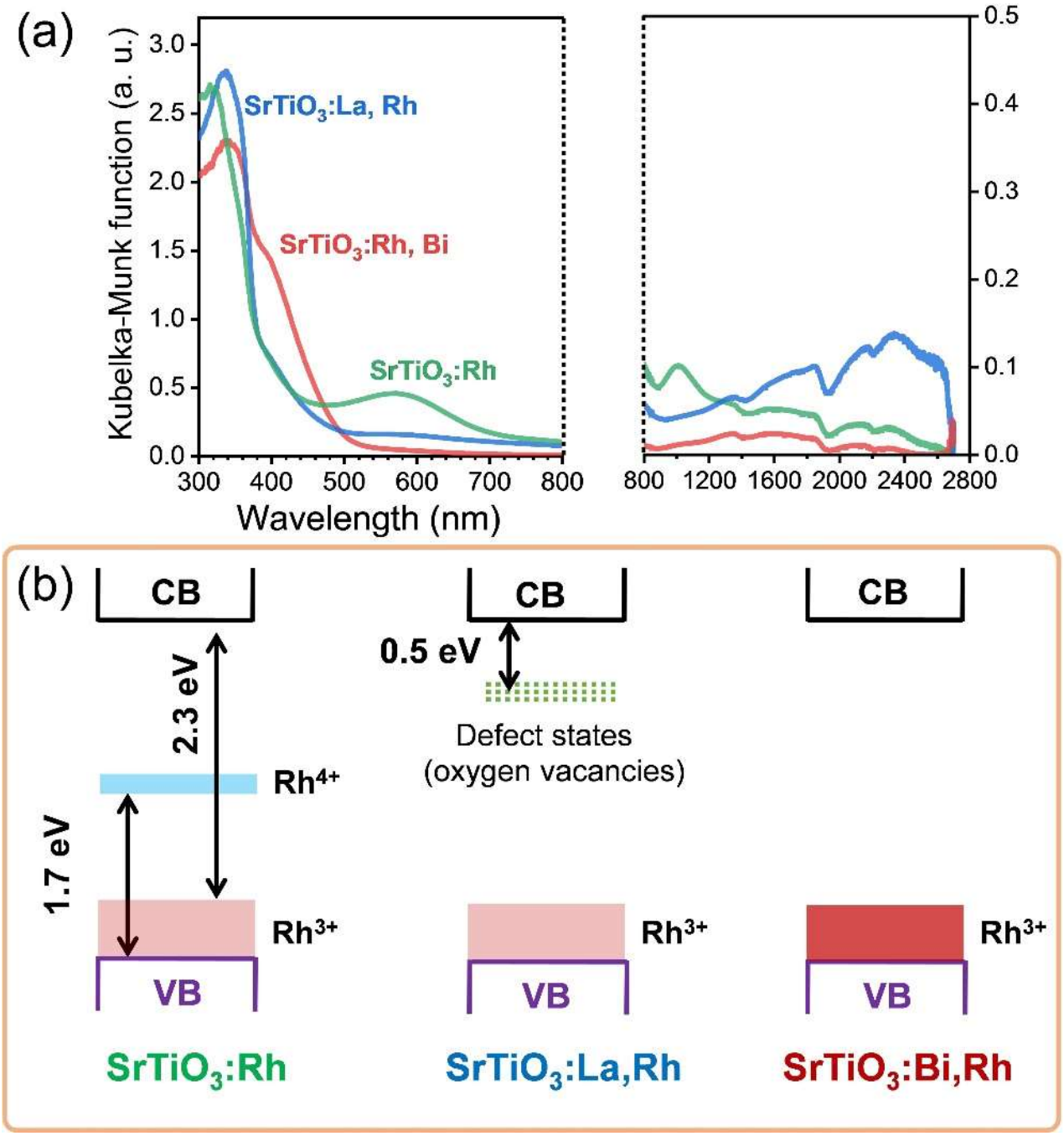

Figure 6. (**a**) DRS spectra, and (**b**) electronic-structure diagrams of $SrTiO_3$:Rh, $SrTiO_3$:La,Rh, and $SrTiO_3$:Bi,Rh [65].

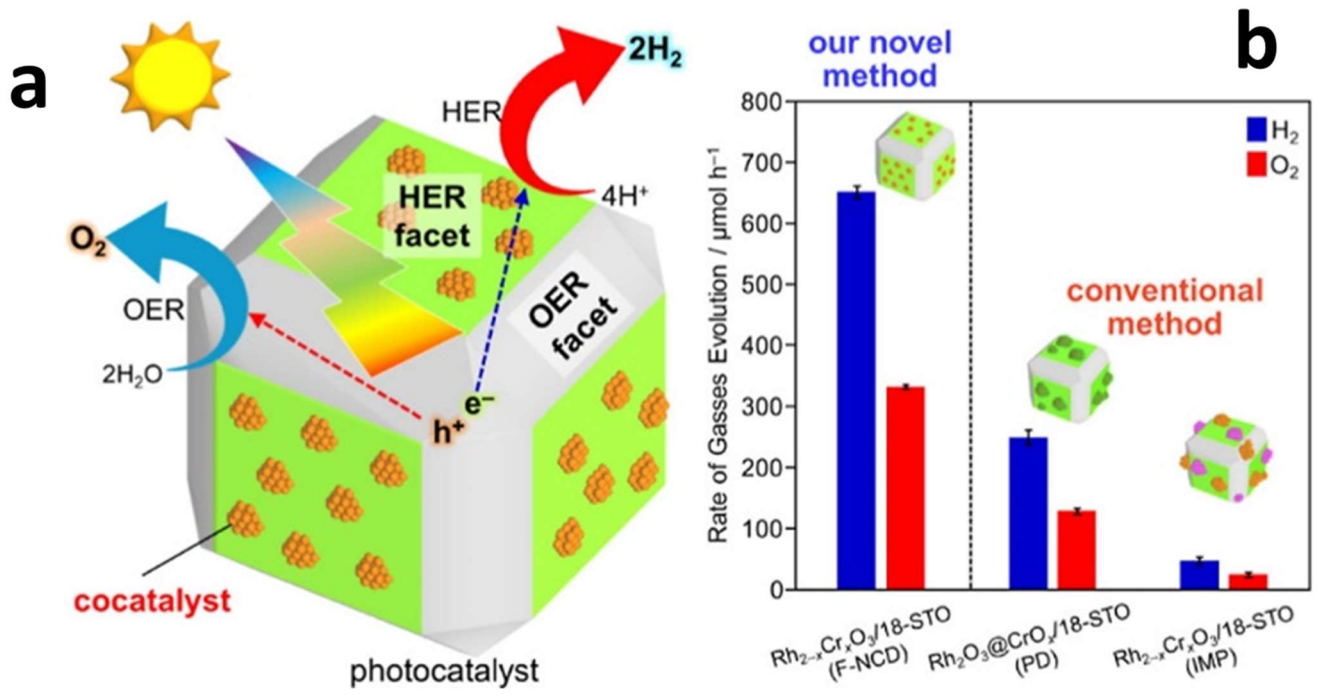

Figure 7. (**a**) Facet based charge transfer mechanism for PCWS (**b**) Comparison of HER and OER [75].

There have been several studies based on noble metals (Pt, Pd, Rh) based cocatalyst loading on photocatalyst for enhanced PCWS. We have done a detailed comparison of recent studies based on AQE, hydrogen production rate, TOF and durability of the photocatalyst in Table 1.

Table 1. Comparison of Noble metal based Cocatalyst studies in the PCWS.

Photocatalyst	Synthesis Method	H_2 Rate ($mmolg^{-1}h^{-1}$)	AQE (%)	Sacrificial Reagent	References
g-C_3N_4/Pt	Thermal polymerizing and photo-deposition	1.2×10^{-3}	0.3	NA	[76]
TiO_2/Pt	In-situ photodeposition	~20	NA	Glycerol	[77]
(0.01–0.5%)Pt/g-C_3N_4	Thermolysis & Chemisorption of Pt	9.4	7.1	TEOA	[78]
CdS/Pt@NU-1000	Ultrasonication & Agitation	3.604	4.57	NaOH	[79]
$BiVO_4$@Pt	Precipitation	115.7×10^{-3}	NA	C_2H=OH	[80]
Pt@C_3N_5	Thermal polymerizing and Ultrasonication	444.2×10^{-3}	0.47	TEOA	[81]
Pt@Tb_4O_7/CN	Hydrothermal & Photo-deposition	132×10^{-3}	5.9	NA	[72]
Pd-TCPP	Solvothermal	21.3	NA	Ascorbic acid	[82]
Pd-CQDs/TiO_2	Hydrothermal & Photo-deposition	11.7	NA	CH_3OH	[73]
Pd@Al:$SrTiO_3$	Molten salt	1.43	38.4	CH_3OH	[83]
Pd@CdS	Hydrothermal and chemical reduction method	18.33	18.5	NA	[84]
R-TAP-Pd(II)@g-C_3N_4	Thermolysis & Ultrasonication	1085×10^{-3}	11.92	TEOA	[85]
Pd@$Ti_3C_2T_x$-TiO_2	Pd loading & Exfoliation	35.11	35.8	NA	[86]
Pd/CuS/Fe_2O_3	Hydrothermal & photodeposition	1120×10^{-3}	NA	TEOA	[87]
Bi_3TiNbO_9/Rh	Hydrothermal & photodeposition	70.45×10^{-3}	0.61	NA	[88]
$SrTiO_3$:Bi:Rh	Molten salt	600×10^{-3}	7.1	CH_3OH	[74]
Rh-Cr_2O_3/STO Facet selective nanocluster deposition	Hydrothermal	650×10^{-3}	2.14	NA	[75]
Rh-NiFeLDH	Hydrothermal	2.09	6.1	Lactic acid	[89]
Rh-Cr-$ZnIn_2S_4$	Hydrothermal & photodeposition	3×10^{-3}	NA	NA	[90]
Rh/GaN-ZnO/Al_2O_3	ALD & photodeposition	50×10^{-3}	7.1	NA	[91]

NA = Not Available.

3.2. Non-Noble Metal Based Cocatalyst for PCWS

Cocatalysts based on noble metals have shown significant potential for addressing energy and climate challenges, but their high costs limit their practical applications. To overcome this, researchers have shifted to non-noble metal-

based cocatalysts, which are more cost-effective, abundant, and possess distinctive properties, making them viable alternatives. Materials like MoS_2, Ni_2P, and CoP have demonstrated remarkable HER activity, while Co_3O_4, NiOOH, and FeOOH excel in OER performance. These cocatalysts play a crucial role in enhancing the stability and durability of photocatalysts under challenging conditions. MoS_2, Ni_2P, and CoP have received considerable attention as HECOs due to their ability to lower the energy barriers for PCWS by acting as electron capturers, thereby reducing charge recombination and boosting HER efficiency. Recent studies have extensively investigated non-noble metal-based cocatalysts, including those containing Co, Ni, W, Fe, and Mo, due to their affordability and ability to form Schottky barriers at metal/semiconductor interfaces. These barriers enhance charge separation and minimize recombination. In water splitting, H^+ ions adsorb onto the cocatalyst surface, where sunlight-activated electrons from the photocatalyst reduce the protons to produce H_2. This section focuses on individual non-noble metal-based cocatalysts, emphasizing their improved HER activity, unique characteristics, and recent advancements in the field.

3.2.1. Ni-Based Cocatalyst for PCWS

Nickel-based cocatalysts play a crucial role in enhancing the efficiency of photocatalytic water splitting by providing active sites for HER and OER. These cocatalysts offer several advantages, including cost-effectiveness, high catalytic activity for HER, resilience under harsh conditions, synergistic properties, tunable electronic characteristics, and reduced overpotential, making them indispensable for PCWS. Various Ni-based cocatalysts, such as Ni metal nanoparticles, Ni_2P, and NiS/Se, have demonstrated exceptional HER activity in aqueous media. Recently, Thabet et al. investigated the loading of Ni cocatalysts onto TiO_2 using different methods, including wet impregnation, hydrothermal, and photocatalytic deposition, with varying weight percentages (0.1–1%), as depicted in Figure 8a–c. The choice of loading method influenced the resulting nanostructures, significantly impacting HER activity. Among these, Ni loaded via the hydrothermal method exhibited the highest hydrogen production, attributed to a shift in absorption towards the visible light region, as shown in Figure 8d [92].

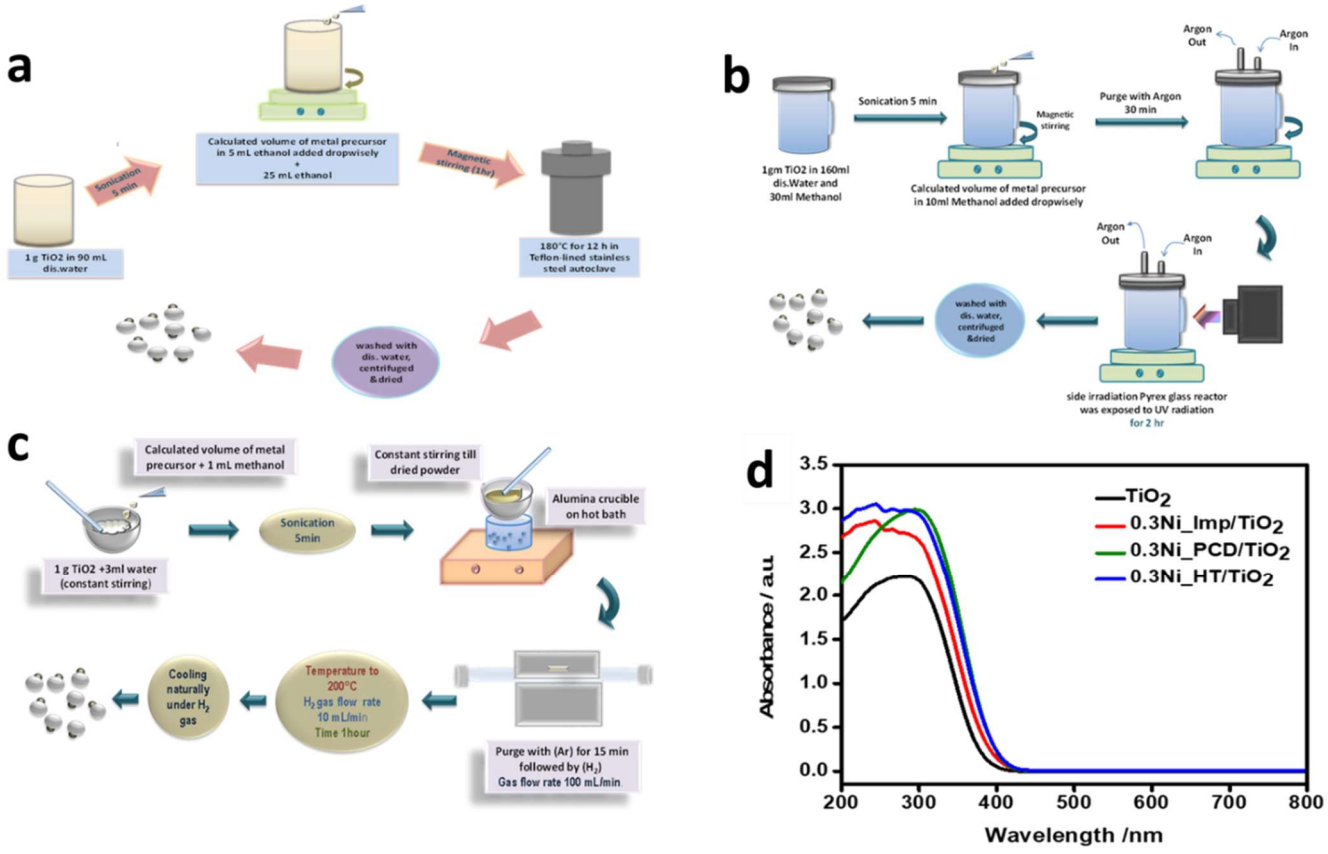

Figure 8. Schematic representation (**a**) Wet impregnation method (**b**) hydrothermal method (**c**) photodeposition method (**d**) 0.3 wt%Ni_TiO_2 with different metal loading methods [92].

The Ni-based cocatalyst Ni_2P has been extensively studied as an efficient cocatalyst due to its notable properties, including excellent electrical conductivity, high catalytic activity for HER, and chemical stability. When combined with semiconducting photocatalysts, Ni_2P provides additional active sites, significantly enhancing HER activity. Recently,

Yiming Lu et al. reported the in-situ deposition of Ni_2P onto CdS for photocatalytic conversion of C_2H_5OH, enabling synergistic H_2 evolution. In this study, Ni_2P was loaded onto CdS using a simple in-situ photodeposition method. Electron Paramagnetic Resonance testing revealed that the presence of Ni_2P enhances the adsorption of hydroxyethyl radicals (*$CH(OH)CH_3$), thereby improving the selectivity of acetaldehyde. This research highlights the importance of cocatalyst loading on bare photocatalysts in improving both the durability and selectivity of reaction products. To further elucidate the enhanced photocatalytic efficiency, the charge transfer mechanism is depicted in Figure 9a. It shows that ethanol oxidation occurs via strongly oxidizing photogenerated holes, producing various products, while water molecules are reduced by electrons to generate hydrogen. Figure 9b provides a comparative analysis of *$CH(OH)CH_3$ based on its relative signal intensity. The results indicate that the Ni_2P-10/CdS composite significantly reduced *$CH(OH)CH_3$ levels in solution compared to pure CdS under equivalent light exposure, demonstrating improved selectivity and efficiency.

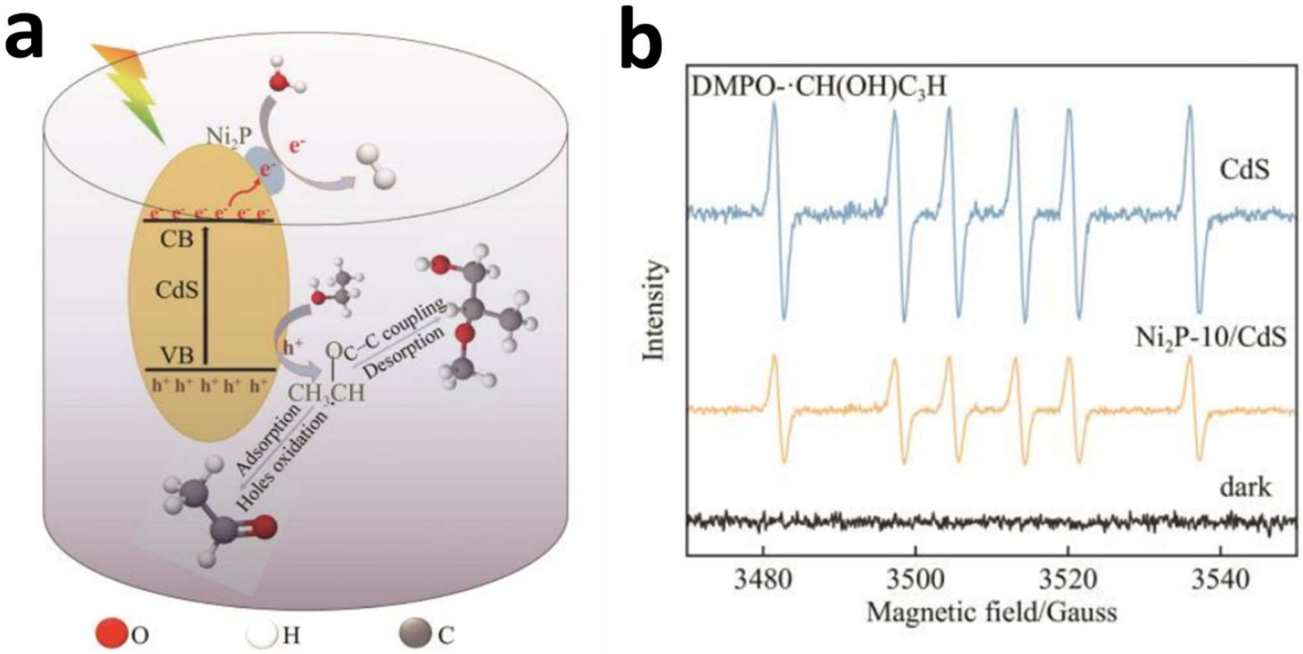

Figure 9. (**a**) Photocatalytic ethanol conversion mechanism of Ni_2P-10/CdS and (**b**) EPR spectra of CdS and Ni_2P-10/CdS [93].

Another Ni-based cocatalyst, Ni_3P_2, has been investigated for its outstanding properties, such as reducing overpotential and enhancing the stability of semiconducting photocatalysts as an HECO in photocatalytic water splitting reactions. In a recent study, Song et al. reported the development of a ZCS/PO/Ni_3P_2 photocatalyst for a three-stage photocatalytic water splitting process to produce H_2 and H_2O_2. The composite material was synthesized using a hydrothermal method followed by a two-step photosynthesis process. The ZCS/PO/Ni_3P_2 composite demonstrated an excellent hydrogen production rate of 9.26 and 9.53 $mmolh^{-1}g^{-1}$ through the oxidation of NaH_2PO_2 in the two-step photosynthesis process. Furthermore, the composite exhibited efficient H_2 and H_2O_2 evolution rates of 1.464 and 1.375 $mmolh^{-1}g^{-1}$, respectively, over 20 h during the PIWS (photocatalytic intermediate water splitting) process. Using a three-stage process of (photocatalytic partial water splitting) PPWS → PPWS → PIWS, a total of 6.88 mmol of H_2 was produced under visible light irradiation within 25 h, corresponding to an average H_2 production rate of 0.28 $mmolh^{-1}$. Notably, this represents the highest reported photocatalytic hydrogen production rate for a $Zn_{1-x}Cd_xS$ composite in PIWS under visible light irradiation. The observed efficiency enhancement is attributed to the charge transfer mechanism, as the composite material demonstrated efficient charge transfer, as illustrated in Figure 10. This study underscores the potential of Ni_3P_2-based cocatalysts in advancing photocatalytic hydrogen production technologies [94].

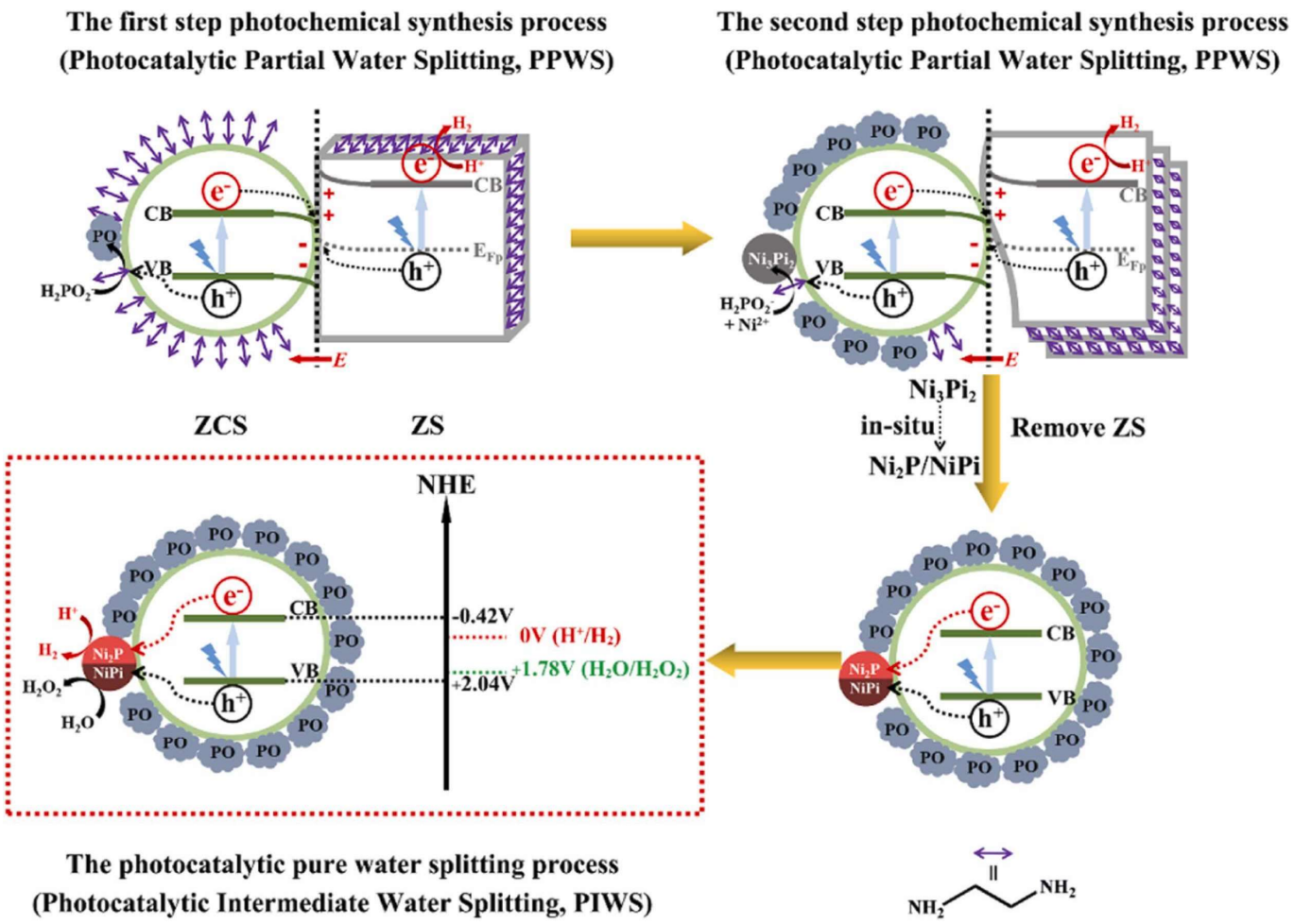

Figure 10. The photocatalytic water splitting mechanism [94].

3.2.2. Co-Based Cocatalyst for PCWS

In addition to Ni-based cocatalysts, Co-based cocatalysts have also been extensively studied as HECOs in photocatalytic water splitting. Co-based materials, including metallic forms, sulfides, and phosphides, have attracted considerable interest due to their ability to reduce overpotential, as well as their stability and regenerative or self-healing properties, making them promising candidates for efficient and durable photocatalytic systems.

The Co-metallic cocatalyst has been extensively studied for its remarkable properties, such as atomic-scale production capabilities and exceptional stability in both acidic and alkaline environments. However, to mitigate light blockage caused by cocatalysts, the development of more transparent alternatives is essential. The photocatalytic response of Co-metallic cocatalysts can be influenced by their morphology and loading amount, making it critical to optimize cocatalyst loading for an efficient system. Morphology is largely determined by the synthesis method and reaction conditions. Due to these properties, Thabet et al. recently reported Co-loaded TiO_2 photocatalysts for enhanced photocatalytic water splitting (PCWS). The Co@TiO_2 photocatalysts were synthesized using different methods, including incipient wet impregnation (Imp), hydrothermal (HT), and photocatalytic deposition (PCD), resulting in distinct morphologies that also affected the TiO_2 band edge in the visible light region, as shown in Figure 11a. The study observed that excessive cocatalyst loading reduced efficiency, likely due to incident light blockage at the photosensitive TiO_2 active sites. Among the methods, Co loaded using the wet impregnation technique exhibited superior performance due to the homogeneous distribution of Co with TiO_2, which enhanced electron capture and reduced charge carrier recombination. The 0.3% Co@TiO_2 prepared via wet impregnation achieved a hydrogen production rate of 16.55 $mmolh^{-1}g^{-1}$, outperforming the 0.3% Co@TiO_2 prepared by HT or PCD methods, as shown in Figure 11b [92].

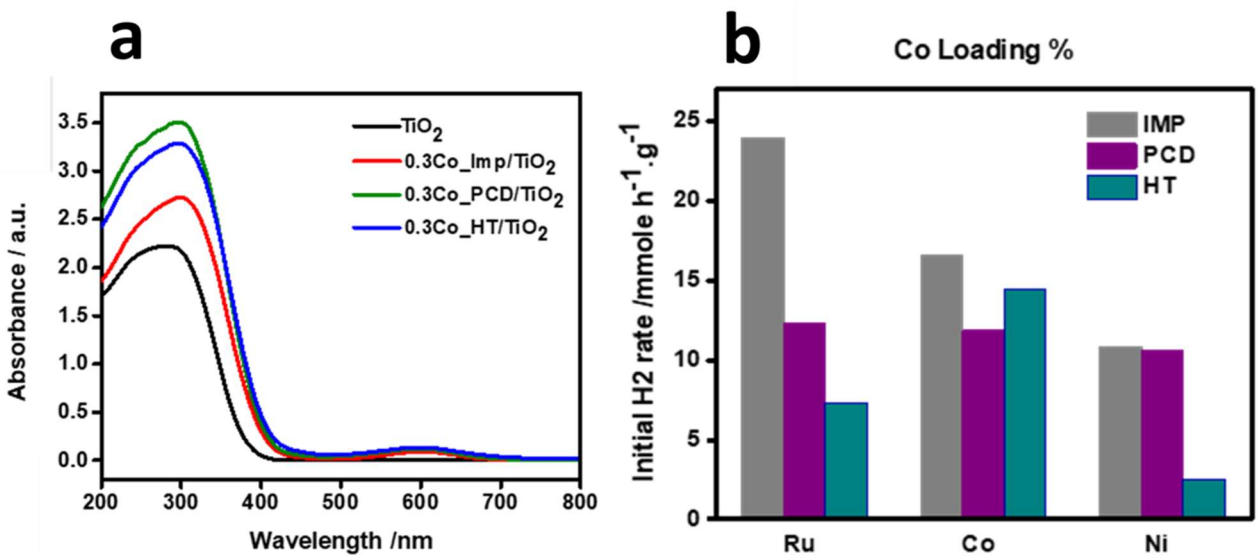

Figure 11. (**a**) UV-Vis DRS spectra for 0.3 wt%Co@TiO_2 (**b**) The relation between initial H_2 production rates and 50 mg of, 0.3 wt%Co@TiO_2, nanocomposites of different metal loading methods [92].

Cobalt-phosphide (CoP) has been extensively studied as an HECO in photocatalytic water splitting (PCWS) due to its self-healing properties, low overpotential, high conductivity, and cost-effectiveness. Its self-healing capability ensures long-term operational stability under harsh acidic or alkaline conditions, making it a promising candidate for PCWS applications. In a recent study, Feitong Zhao et al. investigated a CoP-loaded Mn-doped CdS (MCS) photocatalyst for efficient hydrogen production. Initially, varying amounts of Mn were doped into CdS via a solvothermal method, followed by the deposition–phosphorization of an optimal amount of CoP. The resulting MCS/CoP-7% composite exhibited the highest hydrogen production rate of 40.5 $mmolg^{-1}h^{-1}$, approximately five times higher than that of MCS alone. This enhancement was attributed to the formation of a Schottky heterojunction between MCS and CoP, which facilitated charge transfer and reduced charge recombination. The charge transfer mechanism, illustrated in Figure 12, shows the movement of electrons within the composite. Electrons in the conduction band (CB) of MCS preferentially transfer to CoP due to the lower work function of MCS (3.65 eV) compared to CoP (4.86 eV) [95]. When CoP is used as a cocatalyst on MCS nanorods, its metallic properties enable it to act as an electron trap, effectively capturing electrons from the CB of MCS, thereby enhancing photocatalytic efficiency [96].

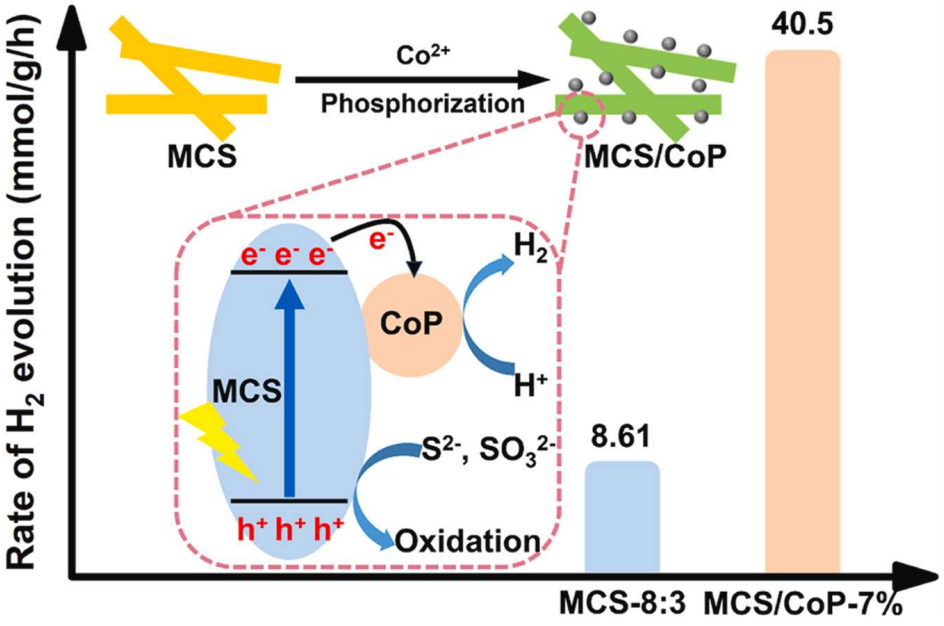

Figure 12. Charge transfer mechanism in MCS/CoP [97].

3.2.3. Mo-Based Cocatalyst for PCWS

Among non-noble metal-based cocatalysts, Mo-based cocatalysts have garnered significant attention for HER reactions in PCWS due to their unique properties. Materials such as MoS_2, MoP, and Mo_2C have been explored for their superior aqueous stability, low overpotential, and abundance of active sites for HER.

MoS_2, in particular, has been widely studied for its layered structure with active edge sites, excellent electrical conductivity, and synergistic interactions with photocatalysts, which enhance HER activity. Its potential to address real-world challenges, such as pollutant degradation and the energy crisis, makes it a highly promising material. A computational study even suggests that MoS_2 exhibits HER activity comparable to that of Pt, highlighting its importance [98]. Building on these features, Wei et al. recently reported the g-C_3N_4@N-MoS_2 photocatalyst for enhanced HER in aqueous media via PCWS [99]. In their study, g-C_3N_4 was prepared through pyrolysis followed by exfoliation at 500 °C to produce ultrathin layers. Subsequently, N-MoS_2 was synthesized via a solvothermal process, where MoS_2 was oxidized to MoO_3 and then subjected to a sulfurization-nitrogenization process to dope it with nitrogen. The introduction of N-sites significantly enhanced the catalytic activity for H^+ reduction on the (002) plane of N-MoS_2. Furthermore, the heterostructure formed between g-$C_3N_4$and N- MoS_2 accelerated HER activity by increasing the exposure of active sites and improving charge separation. Optimal N-MoS_2 doping exhibited the highest H_2 production rate of 360.4 $\mu molg^{-1}h^{-1}$, representing a 19.6 and 14.3-fold increase compared to g-C_3N_4 and 5 wt% MoS_2@g-C_3N_4, respectively. The charge transfer mechanism, illustrated in Figure 13, reveals efficient electron transfer from g-C_3N_4 to the N-MoS_2 cocatalyst surface, facilitating HER.

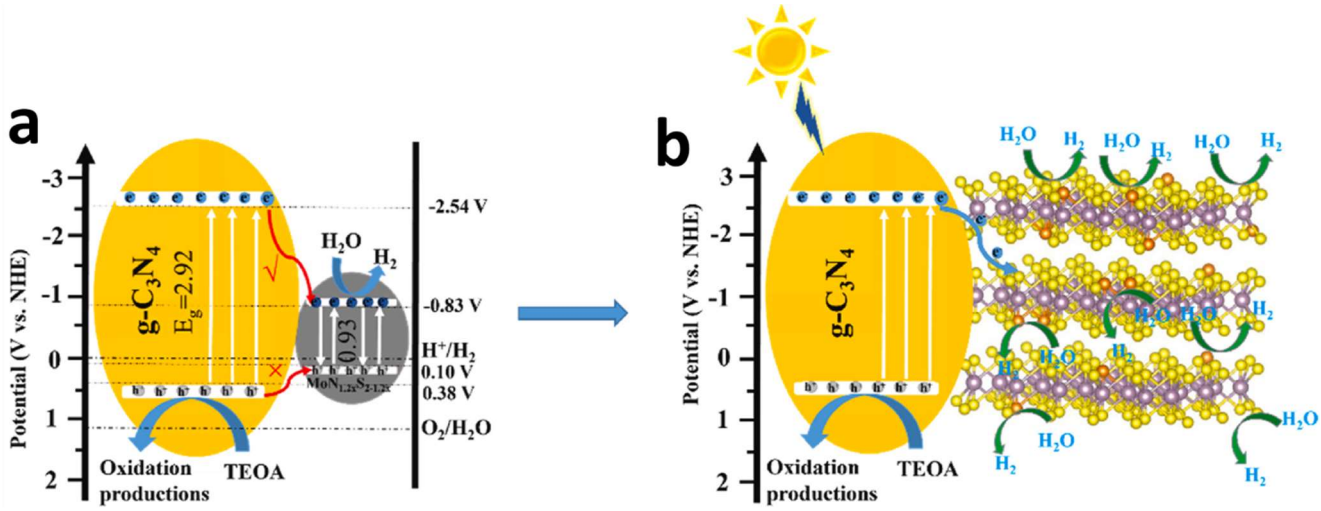

Figure 13. (**a**) The band structures of the $MoN_{1.2x}S_{2-1.2x}$@g-C_3N_4 hybrid and (**b**) The schematic illustration of the proposed mechanism for the photocatalytic H_2 evolution [99].

Other than MoS_2, Mo-based carbides have also gained significant attention for their exceptional HER activity in photocatalytic water splitting. Their excellent electrical conductivity facilitates efficient charge transfer at the photocatalyst-cocatalyst interface, boosting the reaction rate. Additionally, Mo-based carbides exhibit remarkable catalytic activity, reducing charge recombination and lowering the overpotential for HER in PCWS. Their stability under harsh aqueous conditions further highlights their potential for practical applications. The strong interface they form with photocatalysts enhances charge transfer, thereby improving HER efficiency. Inspired by these properties, Yan Wang et al. recently developed a Mo_xC@g-C_3N_4 nanocomposite for enhanced HER in PCWS. The photocatalyst was synthesized by polymerizing melamine at 520 °C for 4 h to produce nanosheets, followed by ultrasound-assisted processing and evaporation. Optimal Mo_xC loading was achieved by varying the temperature during synthesis at 700 °C, 800 °C, and 900 °C. Among these, the nanocomposite Mo_xC700@g-C_3N_4 exhibited the highest H_2 production rate of 7 mmol g^{-1} h^{-1} under identical reaction conditions displayed in Figure 14b. This superior performance is attributed to the formation of a Mo_2C-MoC heterostructure, which facilitates efficient charge transfer and enhances HER activity. The charge transfer mechanism, illustrated in Figure 14a, provides insights into the efficient electron transfer process within the nanocomposite, contributing to the observed enhancement in HER activity.

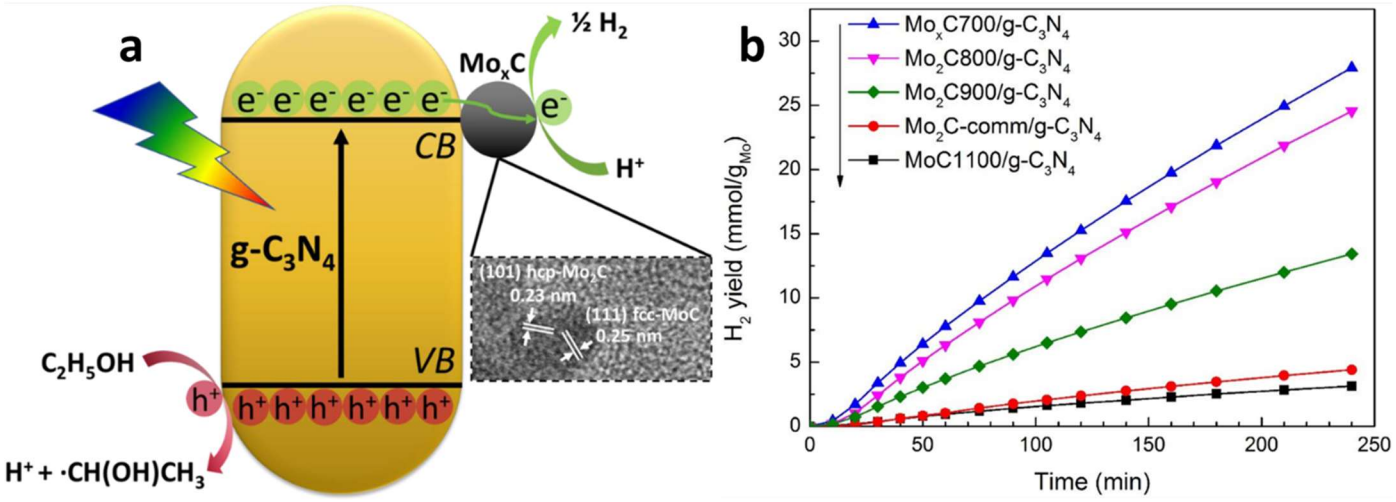

Figure 14. (**a**) Schematic diagram of the photocatalytic H_2 production over $Mo_xC/g\text{-}C_3N_4$ nanocomposites, illustrated for $Mo_xC700/g\text{-}C_3N_4$ [100]; (**b**) H_2 generated per gram of photocatalyst as a function of irradiation time; results from $g\text{-}C_3N_4$ and the blank test are also included. Reaction conditions: 25% *v*/*v* ethanol aqueous solution and $T = 20$ °C.

Non-noble metal Mo-based cocatalysts have demonstrated significant advancements with sulfides and carbides due to their versatile properties. Recently, researchers have expanded their focus to Mo-phosphide (MoP)-based cocatalysts for enhancing HER in photocatalytic water splitting. MoP has been recognized as an efficient cocatalyst for HER, effectively reducing overpotential and accelerating reaction rates. Its Pt-like catalytic behavior makes it an attractive and cost-efficient candidate for practical applications.

MoP exhibits excellent electrical conductivity, enabling efficient charge separation and suppressing charge recombination. It demonstrates high stability in acidic and neutral aqueous media and synergizes well with semiconducting photocatalysts to enhance reaction rates. MoP's surface properties can be tailored to optimize HER activity and its interface with semiconductor photocatalysts. Its favorable H_2 adsorption energy balances the adsorption and desorption of H^+ intermediates during HER. Additionally, MoP plays a dual role as an electron capturer and cocatalyst, accelerating reaction rates while providing stability for real-world applications. Building on these properties, Wang et al. recently developed a TiO_2/MoP/CdS photocatalyst for enhanced H_2 evolution under continuous UV-Vis light irradiation for over 150 h in neutral conditions, demonstrating potential for large-scale operations. The TiO_2/MoP/CdS photocatalyst was prepared by solvothermal synthesis of TiO_2 and CdS, followed by calcination of MoP. The individual components were then combined via ultrasonication to form the composite. This material achieved the highest H_2 production rate of 42.2 $mmol g^{-1} h^{-1}$, 30.1 times greater than that of TiO_2/CdS, making it the most active TiO_2/CdS-based photocatalyst, as shown in Figure 15a. The improved hydrogen production was attributed to a type-II heterojunction mechanism. Electrons transfer from the conduction band (CB) of CdS to MoP and subsequently to the CB of TiO_2, facilitating HER at the TiO_2 surface. Simultaneously, holes migrate in the opposite direction to the CdS surface, enabling OER, as illustrated in Figure 15b. This efficient charge separation and directional transfer significantly enhance the photocatalytic performance [101].The comparison of recent studies based on non-noble metal HECOs is given in Table 2.

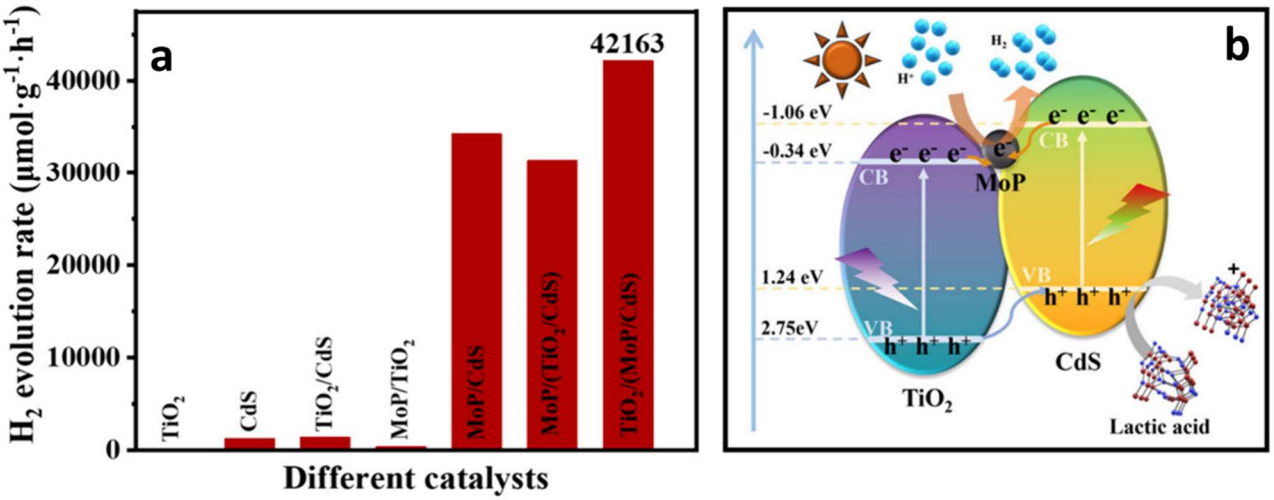

Figure 15. (**a**) H_2 production rate for different photocatalysts (**b**) Possible charge transfer mechanism for HER in The TiO_2/MoP/CdS photocatalyst [101].

Table 2. Comparison of the non-noble metal based cocatalysts for HER in PCWS.

Photocatalyst	Synthesis Method	H_2 Rate ($mmolh^{-1}g^{-1}$)	AQE (%)	Sacrificial Reagent	References
Ni@NiO/$NiCO_3$	*In-situ* thermal treatment	80×10^{-3}	NA	NA	[102]
TiO_2/Ni	Wet Impregnation	10.82	NA	CH_3OH	[92]
CdS/Ni	Hydrothermal	7.4	37.8	C_2H_5OH	[103]
$Zn_2In_2S_5/Ni_2P$	Hydrothermal & Ultrasonic deposition	17.74	NA	TEOA	[104]
CdS/Ni_2P	Hydrothermal & *In-situ* deposition	2.2	NA	C_2H_5OH	[93]
CdS/Ni_2P	Hydrothermal & Ultrasonic deposition	4.34	NA	TEOA	[105]
ZCS/PO/Ni_3Pi_2	Hydrothermal & Photosynthesis	1.45	1.86	NA	[94]
CdS/Co	Hydrothermal & Photodeposition	26	NA	$(NH_4)_2SO_3$	[106]
g-C_3N_4/Co	Thermal treatment & Photodeposition	2.3	6.2	TEOA	[107]
P-g-C_3N_4/Co	*In-situ* thermal treatment	892.5×10^{-3}	NA	TEOA	[108]
CoP/Mn-CdS	Hydrothermal & Deposition–phosphorization	40.5	19.6	Na_2SO_3/Na_2S	[97]
CoP/Ni-CdS	Hydrothermal & Calcination	42.14	16.8	Na_2SO_3/Na_2S	[109]
CoP/$ZnIn_2S_4$	Hydrothermal & Phosphorization	4.24	NA	TEOA	[110]
CdS/MoS_2	Hydrothermal	31.09	NA	Lactic acid	[111]
MoS_2/g-$C_3N_4/ZnIn_2S_4$	Hydrothermal	5.6	13.6	TEOA	[112]
MoC/NC-CdS	Hydrothermal & *In-situ* deposition	11.4	13.38	Formic acid	[113]
MoC-Q3/g-C_3N_4	Ultrasonication and heating	50.1	NA	TEOA	[114]
MoP/SiC	Hydrothermal	589.23×10^{-3}	27.6	Ethylene glycol	[115]
$ZnIn_2S_4$/MoP	Solvothermal	2.03	10.5	Na_2SO_3/Na_2S	[116]

NA = Not Available.

3.3. Metal Free Cocatalyst

As previously discussed, noble and non-noble metal-based cocatalysts have shown significant potential for large-scale applications in addressing energy crises and climate change. However, the environmental concerns associated with metal-based cocatalysts, including the risk of photocorrosion, have driven researchers to explore alternative solutions. Metal-free cocatalysts have recently gained attention as a promising alternative. Composed of elements like boron (B), carbon (C), phosphorus (P), and nitrogen (N), these cocatalysts are eco-friendly and highly robust, making them well-suited for use under severe conditions in real-world applications. While metal-free cocatalysts have been less extensively studied compared to their metal-based counterparts, they hold significant potential for further exploration and development. Notable examples of well-studied metal-free cocatalysts include polyaniline (PANI), polypyrrole (PPy), and graphene quantum dots (GQDs). In this section, we will focus on the role of GQDs, PPy, and PANI cocatalysts in photocatalytic water splitting (PCWS) and their contributions to enhancing HER activity.

The PANI cocatalyst has been extensively studied due to its unique properties as a highly conductive polymer, which facilitates efficient charge transfer between the photocatalyst and reaction sites, thereby suppressing charge recombination. Its structure includes nitrogen (N) atoms, which can act as active sites for HER by adsorbing and

stabilizing H^+ ions. Furthermore, PANI exhibits excellent stability under acidic and neutral aqueous conditions, essential for HER activity. Acting as an electron capturer, PANI reduces charge recombination and accelerates HER reaction rates, making it a promising candidate for real-world applications. Due to its dynamic properties, PANI has been widely explored in photoelectrochemical (PEC) and photocatalytic water splitting (PCWS) systems for HER. Recently, Sindhu et al. reported a novel V, S co-doped Ta_3N_5 photocatalyst protected with a PANI composite for enhanced hydrogen production. This study explored the synergistic effect of the conductive polymer and the doped semiconductor photocatalyst. The V, S co-doped Ta_3N_5 photocatalyst was prepared via a two-step method: ball milling (V_2O_5 + Ta_3N_5) followed by calcination. Sulfur (S) doping was achieved by adding urea as a sulfur source. The PANI was synthesized separately through the polymerization of aniline. To form the composite, the V, S-Ta_3N_5 and PANI were mixed using ultrasonication. The resulting composite material demonstrated a hydrogen production rate of 98.4 $\mu molg^{-1}h^{-1}$, significantly outperforming other photocatalysts, as shown in Figure 16a [117]. The enhanced hydrogen production was attributed to the efficient charge transfer facilitated by the modified electronic structure of the pristine Ta_3N_5, which was optimized through V and S doping. The subsequent PANI loading was further contributed to timely capturing electrons, effectively reducing charge recombination, as illustrated in Figure 16b. This combination of properties highlights the potential of PANI-based composites in advancing HER applications.

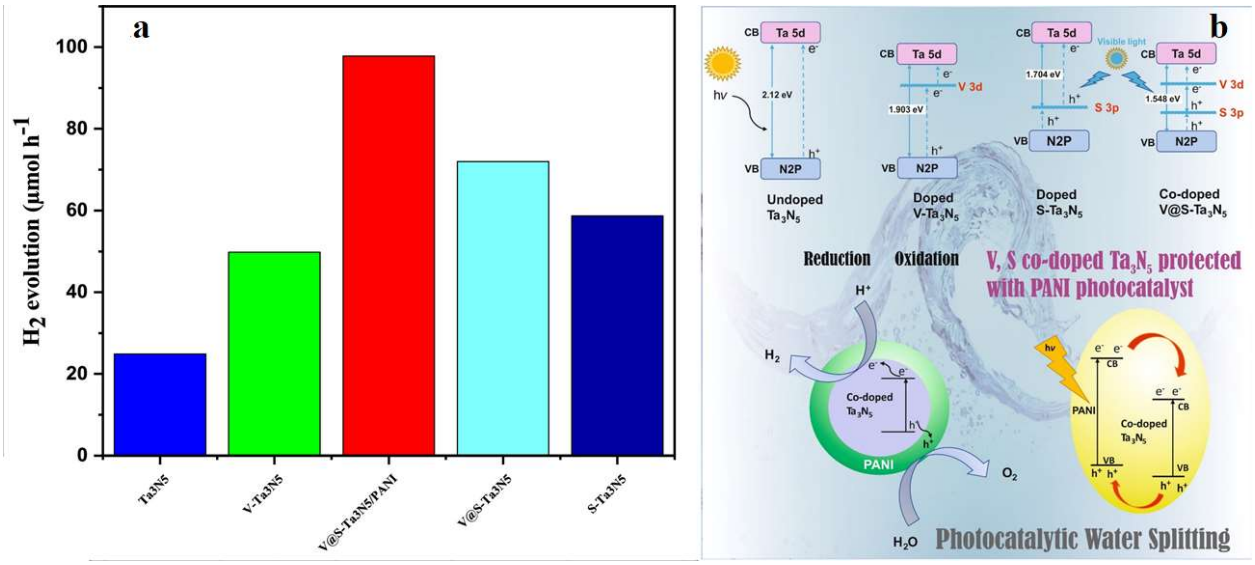

Figure 16. (**a**) The H_2 evolution activity of the pristine Ta_3N_5, and the synthesized materials V-doped Ta_3N_5, S-Ta_3N_5, and V@S codoped-Ta_3N_5 (**b**) Schematic representation of the possible mechanism for the evolution of H_2 via the photocatalytic process [117].

In addition to PANI, polypyrrole (PPy) has also been extensively explored as an HECO due to its ability to tune the photocatalyst bandgap, enhance visible light absorption, and provide high mechanical strength and electrical conductivity. PPy exhibits excellent stability in acidic and neutral media, biocompatibility due to its intrinsic continuous π-conjugation, and nanoscale dimensions, making it an efficient cocatalyst for H_2 production through PCWS [118]. Owing to these dynamic properties, Ghosh et al. recently reported a mixed copper-cuprous oxide (CuO/Cu_2O) composite with PPy for enhanced hydrogen production in PCWS. The composite was synthesized through a simple in-situ oxidative polymerization method. The integration of mixed CuO/Cu_2O with PPy extended light absorption into the visible spectrum, as illustrated in Figure 17a, resulting in a 7-fold increase in H_2 production compared to other photocatalysts. The enhanced performance was attributed to reduced charge recombination, a higher number of free charge carriers, an increased number of active HER sites, and intimate contact between PPy nanofibers and the CuO/Cu_2O interface. The charge transfer mechanism responsible for this improvement involves the formation of a p-n heterojunction between Cu_2O and CuO, and a p-p heterojunction between CuO and PPy. These heterojunctions facilitate charge transfer via upward and downward band bending, forming a space-charge layer and generating an internal electric field that supports efficient charge transfer. Additionally, PPy plays a critical role under sunlight by inducing a π–π* electron transition from its valence band (VB) to the conduction band (CB), with these excited electrons quickly transferring to the CB of mixed CuO/Cu_2O. This process, along with the overall charge transfer mechanism, is schematically detailed in Figure 17b, highlighting the role of PPy in boosting PCWS efficiency.

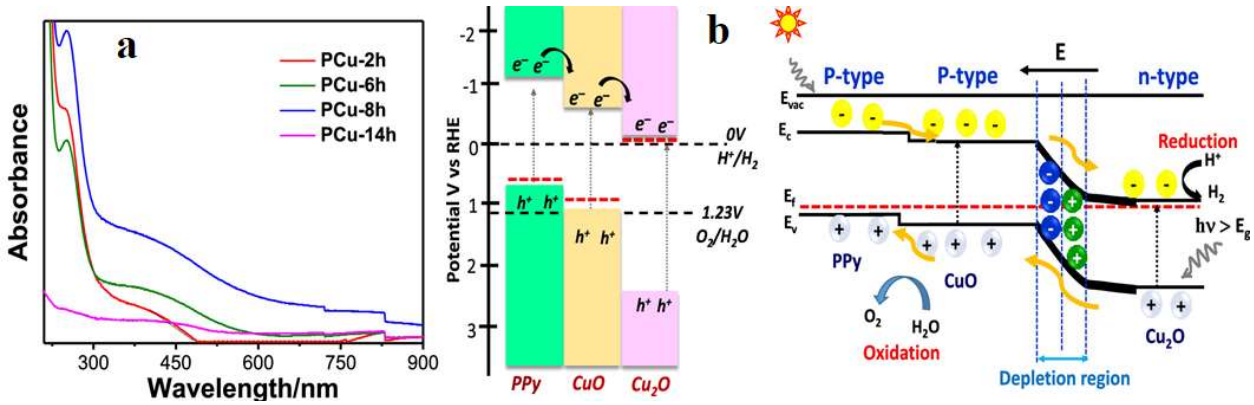

Figure 17. (**a**) UV-Vis spectra for mixed copper/cuprous with PPy cocatalyst loading for different time. (**b**) Bandedge structure and charge transfer mechanism [119].

Graphene Quantum Dots (GQDs) have also been explored as cocatalysts for HER in photocatalytic water splitting (PCWS) due to their unique properties. GQDs exhibit high stability in aqueous conditions, excellent electrical conductivity, active sites for H^+ adsorption, and 3D electron confinement, which collectively enhance HER activity. Additionally, GQDs possess low toxicity and tunable fluorescence emission properties, making them highly versatile [120]. In a recent study, Raghavan et al. reported the development of GQDs-loaded TiO_2 composites for enhanced hydrogen production in PCWS. The TiO_2@GQDs composite was synthesized using a hydrothermal method, with P-25 serving as the TiO_2 source. GQDs were fabricated through ultrasonic fragmentation of graphene. Optimization of GQDs loading revealed that a 15% GQDs loading on TiO_2, designated CNTP-3, yielded the best results. The P-25 TiO_2, containing both rutile and anatase phases, also played a critical role in achieving the enhanced hydrogen production rate. The CNTP-3 composite achieved a remarkable hydrogen production rate of 29,548 $\mu molg^{-1}h^{-1}$, significantly outperforming pristine TiO_2, as depicted in Figure 18a. The enhanced performance was attributed to efficient charge transfer facilitated by the synergistic interaction between GQDs and TiO_2, which minimized charge recombination. The charge transfer mechanism, thoroughly detailed in Figure 18b, highlights the role of GQDs in improving electron mobility and facilitating HER at the composite interface, making GQDs-loaded TiO_2 a promising system for PCWS applications [121]. The comparison of recent studies based on metal free HECOs is given in Table 3.

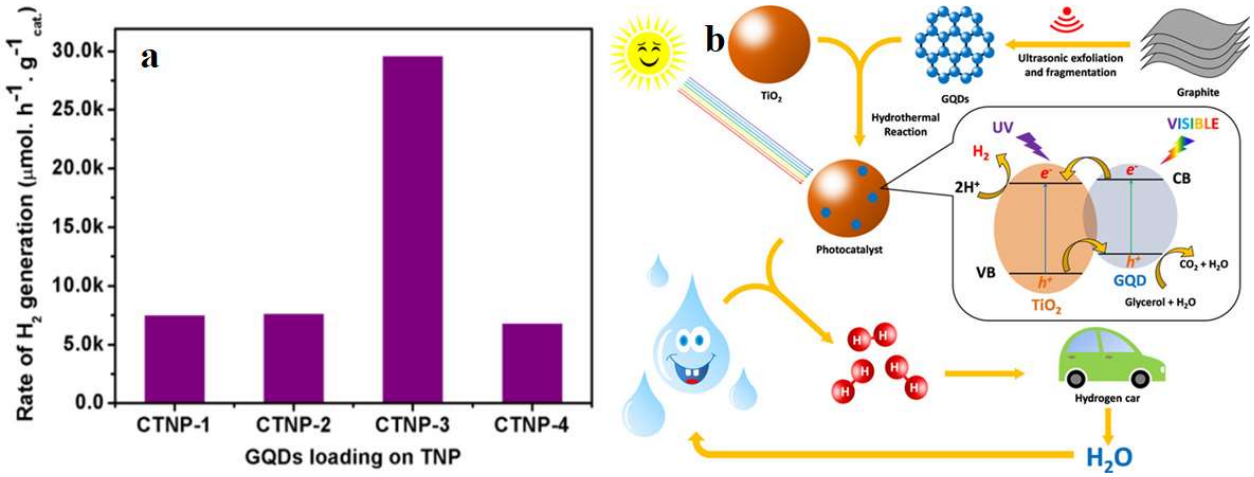

Figure 18. (**a**) Rate of H_2 generation by GQD-TNP composites with different weight percentages of GQDs. (**b**) Charge transfer mechanism [121].

Table 3. Comparison of metal free HECO in PCWS.

Photocatalyst	Synthesis Method	H_2 Rate ($mmolh^{-1}g^{-1}$)	AQE (%)	Sacrificial Reagent	References
Nb-Ta_3N_5 @PANI	Ultrasonication & calcination	71.3	NA	NA	[122]
V,S-Ta_3N_5 @PANI	Ball-milling mixing & Chemisorption	98.4	NA	NA	[117]
Ta_3N_5/BSC@PANI	Ball-milling mixing & Chemisorption	76.9×10^{-3}	NA	CH_3OH	[123]
PANI/BiOCl/GO	Oxidative polymerization	1000×10^{-6}	17.97	CH_3OH	[124]
Pani@rGO/CuO	Hydrothermal	16.7	NA	CH_3OH	[125]
Cu_6Sn_5/PANI	Chemical reduction and hydrothermal	121.3×10^{-3}	NA	NA	[126]
Cd-ZnS/PANI	Hydrothermal	721×10^{-3}	30.2	Na_2S/Na_2SO_3	[127]

CeO_2/PPy/BFO	Hydrothermal and coprecipitation	18.5	NA	CH_3OH	[128]
CeO_2/PPy	Hydrothermal and coprecipitation	8.4	NA	CH_3OH	[128]
ZnO/PPy	Polymerization & Wet Impregnation	162	16.1	CH_3OH	[129]
TiO_2/PPy	Polymerization & Wet Impregnation	76	7.5	CH_3OH	[129]
PPy/ZnO	Etching	11.62×10^{-3}	NA	Na_2S/Na_2SO_3	[130]
$ZnFe_2O_4$@WO_{3-x}/PPy	Hydrothermal	657×10^{-3}	NA	CH_3OH	[131]
$ZnIn_2S_4$/PPy	Ultrasonication & Low temp rotation	1200×10^{-3}	6.43	NA	[132]
GQDs/Bi_2S_3	Hydrothermal	869.12×10^{-3}	NA	IPA	[133]
Cu-TiO_2/CQDs	MW-assisted	7.2×10^{-3}	NA	CH_3OH	[134]
SN-GQDs/TiO_2	Hydrothermal	19.2	NA	CH_3OH	[135]
MoS_2/ZIS/GQDs	Hydrothermal	21.63	15.19	Ascorbic Acid	[136]
g-C_3N_4/N-GQDs	Thermolysis & Hydrothermal	1.1	NA	TEOA	[137]
TiO_2/GQDs	Hydrothermal	2.2×10^{-3}	NA	C_2H_5OH	[138]

NA = Not Available.

4. Conclusions and Future Perspectives

Photocatalytic water splitting (PCWS) holds immense promise for addressing renewable energy challenges, such as green hydrogen production and mitigating climate change. However, significant hurdles remain, including limited long-term stability, high charge recombination rates, low hydrogen production efficiency, restricted apparent quantum efficiency (AQE), and low turnover frequency (TOF). Recent studies have emphasized the critical role of cocatalysts in enhancing HER activity in PCWS, highlighting the need for periodic reviews to guide future research effectively. In this review, we examined various cocatalyst loading processes and their roles in improving HER activity, focusing on the fundamental aspects of cocatalysts in PCWS. We provided detailed insights into charge transfer mechanisms between cocatalysts and photocatalysts under challenging conditions. The discussion included noble metal-based cocatalysts (e.g., Pt, Pd, Rh), non-noble metal cocatalysts (e.g., Ni_2S, Ni_2P, Ni_3P_2, MoP, Mo_2C, MoS_2, CoP, Co_xS), and metal-free cocatalysts (e.g., PANI, PPy, GQDs). Our findings underline the critical role cocatalysts play in enhancing stability, improving synergistic interactions with photocatalysts, and accelerating HER reaction rates. HECOs effectively capture electrons and reduce charge recombination, making them indispensable for achieving higher efficiency in PCWS. This review aims to provide comprehensive and conclusive resource for researchers in the field.

Though cocatalyst loading significantly enhances HER efficiency and stability, achieving optimal hydrogen production cannot rely solely on this strategy. Challenges remain in tuning the semiconductor band edge and creating suitable interfaces for large-scale H_2 production. Several strategies, such as shifting the band edge into the visible light region, forming passivation layers, and designing Schottky junctions between semiconductors and cocatalysts, must be further explored. The development of core-shell structures and hybrid 2D/3D systems should be prioritized to address energy and climate challenges effectively. Additionally, self-healing cocatalysts like CoP and metal-free cocatalysts require deeper investigation to unlock their full potential. Advancing fabrication techniques to create stable and efficient cocatalysts under severe conditions is essential for overcoming current limitations and realizing the full potential of PCWS for sustainable energy solutions.

Acknowledgments

The authors acknowledge University of Cincinnati for providing research infrastructure.

Author Contributions

B.M.: Original draft, Writing—review and editing. P.C.M.: Review and editing. P.G.S.: Supervision, review and editing.

Ethics Statement

Not applicable.

Informed Consent Statement

Not applicable.

Data Availability Statement

The data used in the review can be accessed through the cited publication within the manuscript.

Funding

This research received no external funding.

Declaration of Competing Interest

The authors declare that they have no known competing financial interests or personal relationships that could have appeared to influence the work reported in this paper.

Dedication

This paper is dedicated to Professor David F. Ollis, who left us on 6 October 2023. Renowned internationally, Professor Ollis was a pioneer in chemical engineering and technology, making groundbreaking contributions that reshaped the field. His research was marked by remarkable depth and diversity. He played a key role in introducing Biochemical Engineering to most Chemical Engineering departments across the United States and many other countries. Beyond his exceptional research, he was a devoted teacher who deeply cared for his students and their education. As a dear friend and mentor to me (PGS), Professor Ollis will be greatly missed, but his legacy and work will endure.

References

1. Staffell I, Scamman D, Velazquez Abad A, Balcombe P, Dodds PE, Ekins P, et al. The Role of Hydrogen and Fuel Cells in the Global Energy System. *Energy Environ. Sci.* **2019**, *12*, 463–491. doi:10.1039/C8EE01157E.
2. Rajeshwar K. Solar Energy Conversion and Environmental Remediation Using Inorganic Semiconductor–Liquid Interfaces: The Road Traveled and the Way Forward. *J. Phys. Chem. Lett.* **2011**, *2*, 1301–1309. doi:10.1021/jz200396h.
3. Colmenares JC, Luque R. Heterogeneous Photocatalytic Nanomaterials: Prospects and Challenges in Selective Transformations of Biomass-Derived Compounds. *Chem. Soc. Rev.* **2014**, *43*, 765–778. doi:10.1039/C3CS60262A.
4. Colmenares JC, Luque R, Campelo JM, Colmenares F, Karpiński Z, Romero AA. Nanostructured Photocatalysts and Their Applications in the Photocatalytic Transformation of Lignocellulosic Biomass: An Overview. *Materials* **2009**, *2*, 2228–2258. doi:10.3390/ma2042228.
5. Qu Y, Duan X. Progress, Challenge and Perspective of Heterogeneous Photocatalysts. *Chem. Soc. Rev.* **2013**, *42*, 2568–2580. doi:10.1039/C2CS35355E.
6. Kaushal N, Taha AA, Tyagi S, Smirniotis PG. NH2-MIL-101(Fe)/N-CNDs as a Visible Light Photocatalyst for Degradation of Fluoroquinolone Antibiotics in Water. *Mater. Chem. Phys.* **2025**, *332*, 130198. doi:10.1016/j.matchemphys.2024.130198.
7. Sun B, Vorontsov AV, Smirniotis PG. Role of Platinum Deposited on TiO_2 in Phenol Photocatalytic Oxidation. *Langmuir* **2003**, *19*, 3151–3156. doi:10.1021/la0264670.
8. Sun B, Reddy EP, Smirniotis PG. Visible Light Cr(VI) Reduction and Organic Chemical Oxidation by TiO_2 Photocatalysis. *Environ. Sci. Technol.* **2005**, *39*, 6251–6259. doi:10.1021/es0480872.
9. Du P, Eisenberg R. Catalysts Made of Earth-Abundant Elements (Co, Ni, Fe) for Water Splitting: Recent Progress and Future Challenges. *Energy Environ. Sci.* **2012**, *5*, 6012–6021. doi:10.1039/C2EE03250C.
10. Skov AM. World Energy Beyond 2050. In Proceedings of the SPE Annual Technical Conference and Exhibition, San Antonio, TX, USA, 29 September–2 October 2002; p SPE-77506-MS. doi:10.2118/77506-MS.
11. Papantonis D, Stavrakas V, Tzani D, Flamos A. Towards Decarbonisation or Lock-in to Natural Gas? A Bottom-up Modelling Analysis of the Energy Transition Ambiguity in the Residential Sector by 2050. *Energy Convers. Manag.* **2025**, *324*, 119235. doi:10.1016/j.enconman.2024.119235.
12. Permude P, Tang C, Ahmad A, Chen H, Frankcombe T, Liu Y. Effective Catalysts for Typical Liquid Organic Hydrogen Carrier N-Ethylcarbazole. *Int. J. Hydrogen Energy* **2025**, *98*, 1492–1509. doi:10.1016/j.ijhydene.2024.12.038.
13. Züttel A, Remhof A, Borgschulte A, Friedrichs O. Hydrogen: The Future Energy Carrier. *Philos. Trans. R. Soc. A Math. Phys. Eng. Sci.* **2010**, *368*, 3329–3342. doi:10.1098/rsta.2010.0113.
14. Li L, Wang P, Shao Q, Huang X. Metallic Nanostructures with Low Dimensionality for Electrochemical Water Splitting. *Chem. Soc. Rev.* **2020**, *49*, 3072–3106. doi:10.1039/D0CS00013B.
15. Li X, Hao X, Abudula A, Guan G. Nanostructured Catalysts for Electrochemical Water Splitting: Current State and Prospects. *J. Mater. Chem. A* **2016**, *4*, 11973–12000. doi:10.1039/C6TA02334G.
16. Wang J, Cui W, Liu Q, Xing Z, Asiri AM, Sun X. Recent Progress in Cobalt-Based Heterogeneous Catalysts for Electrochemical Water Splitting. *Adv. Mater.* **2016**, *28*, 215–230. doi:10.1002/adma.201502696.
17. Subramanyam P, Meena B, Biju V, Misawa H, Challapalli S. Emerging Materials for Plasmon-Assisted Photoelectrochemical Water Splitting. *J. Photochem. Photobiol. C Photochem. Rev.* **2022**, *51*, 100472. doi:10.1016/j.jphotochemrev.2021.100472.
18. Meena B, Kumar M, Gupta S, Sinha L, Subramanyam P, Subrahmanyam C. Rational Design of $TiO_2/BiSbS_3$ Heterojunction for Efficient Solar Water Splitting. *Sustain. Energy Technol. Assess.* **2022**, *49*, 101775. doi:10.1016/j.seta.2021.101775.

19. Meena B, Kumar M, Subramanyam P, Nagumothu R, Smith D, Juodkazis S, et al. Optimal Deposition of a Thin FeOOH Layer on S-TiO_2/$BiSbS_3$ p-n Junction for Improved Solar Water Splitting and Mechanistic Insights. *Mater. Res. Bull.* **2023**, *168*, 112493. doi:10.1016/j.materresbull.2023.112493.
20. Joy R, Meena B, Kumar M, Jospeh M, Joseph S, Subrahmanyam C, et al. Exploring the Role of ZnS as Passivation Layer on $SrTiO_3$/Bi_2S_3 Heterojunction Photoanode for Improved Solar Water Splitting. *Catal. Today* **2024**, *433*, 114669. doi:10.1016/j.cattod.2024.114669.
21. Joseph M, Meena B, Joy R, Joseph S, Sethi RK, Remello SN, et al. Rational Design of a G-C_3N_4/Bi_2S_3/ZnS Ternary Heterojunction Photoanode for Improved Solar Water Splitting. *Sustain. Energy Fuels* **2024**, *8*, 3412–3418. doi:10.1039/D4SE00147H.
22. Meena B, Subramanyam P, Suryakala D, Biju V, Subrahmanyam C. Efficient Solar Water Splitting Using a CdS Quantum Dot Decorated TiO_2/Ag_2Se Photoanode. *Int. J. Hydrogen Energy* **2021**, *46*, 34079–34088. doi:10.1016/j.ijhydene.2021.07.219.
23. Kumar KVA, Chandana L, Ghosal P, Subrahmanyam C. Simultaneous Photocatalytic Degradation of P-Cresol and Cr (VI) by Metal Oxides Supported Reduced Graphene Oxide. *Mol. Catal.* **2018**, *451*, 87–95. doi:10.1016/j.mcat.2017.11.014.
24. Daya Mani A, Muthusamy S, Anandan S, Subrahmanyam C. C and N Doped Nano-Sized TiO_2 for Visible Light Photocatalytic Degradation of Aqueous Pollutants. *J. Exp. Nanosci.* **2015**, *10*, 115–125. doi:10.1080/17458080.2013.803613.
25. Maeda K. Photocatalytic Water Splitting Using Semiconductor Particles: History and Recent Developments. *J. Photochem. Photobiol. C Photochem. Rev.* **2011**, *12*, 237–268. doi:10.1016/j.jphotochemrev.2011.07.001.
26. Maeda K, Domen K. Photocatalytic Water Splitting: Recent Progress and Future Challenges. *J. Phys. Chem. Lett.* **2010**, *1*, 2655–2661. doi:10.1021/jz1007966.
27. Fujishima A, Honda K. Electrochemical Photolysis of Water at a Semiconductor Electrode. *Nature* **1972**, *238*, 37–38. doi:10.1038/238037a0.
28. Takanabe K. Photocatalytic Water Splitting: Quantitative Approaches toward Photocatalyst by Design. *ACS Catal.* **2017**, *7*, 8006–8022. doi:10.1021/acscatal.7b02662.
29. Li R, Li C. Chapter One—Photocatalytic Water Splitting on Semiconductor-Based Photocatalysts. In *Advances in Catalysis*; Song CBT-A, Ed.; Academic Press: Cambridge, MA, USA, 2017; Volume 60, pp. 1–57. doi:10.1016/bs.acat.2017.09.001.
30. Acar C, Dincer I, Naterer GF. Review of Photocatalytic Water-Splitting Methods for Sustainable Hydrogen Production. *Int. J. Energy Res.* **2016**, *40*, 1449–1473. doi:10.1002/er.3549.
31. Fajrina N, Tahir M. A Critical Review in Strategies to Improve Photocatalytic Water Splitting towards Hydrogen Production. *Int. J. Hydrogen Energy* **2019**, *44*, 540–577. doi:10.1016/j.ijhydene.2018.10.200.
32. Yeh T-F, Cihlář J, Chang C-Y, Cheng C, Teng H. Roles of Graphene Oxide in Photocatalytic Water Splitting. *Mater. Today* **2013**, *16*, 78–84. doi:10.1016/j.mattod.2013.03.006.
33. Gomathi Devi L, Shyamala R. Photocatalytic Activity of SnO_2–α-Fe_2O_3 Composite Mixtures: Exploration of Number of Active Sites, Turnover Number and Turnover Frequency. *Mater. Chem. Front.* **2018**, *2*, 796–806. doi:10.1039/C7QM00536A.
34. Kisch H, Bahnemann D. Best Practice in Photocatalysis: Comparing Rates or Apparent Quantum Yields? *J. Phys. Chem. Lett.* **2015**, *6*, 1907–1910. doi:10.1021/acs.jpclett.5b00521.
35. Kumar M, Kuttasseri A, Meena B, Mahata A, Challapalli S. Synergetic NIR Responsive Plasmonic CuxS Nanodisks on CuO Photocathodes for Photo-Electrochemical Water Splitting. *Appl. Catal. B Environ. Energy* **2024**, *357*, 124317. doi:10.1016/j.apcatb.2024.124317.
36. Cho PP, Mon PP, Kumar M, Madras G, Subrahmanyam C. Rational Bi-MoO Nanospheres Decorated g-C_3N_4 for Photocatalytic Performance of Dye Degradation. *Surf. Interfaces* **2024**, *50*, 104522. doi:10.1016/j.surfin.2024.104522.
37. Prabhu A, Meenu PC, Roy S. Creation of a Facile Heterojunction in Co/ZnO–TiO_2 for the Photocatalytic Degradation of Alizarin S. *New J. Chem.* **2024**, *48*, 10552–10562. doi:10.1039/D4NJ00407H.
38. Li Y, Hou Y, Fu Q, Peng S, Hu YH. Oriented Growth of $ZnIn_2S_4$/$In(OH)_3$ Heterojunction by a Facile Hydrothermal Transformation for Efficient Photocatalytic H_2 Production. *Appl. Catal. B Environ.* **2017**, *206*, 726–733. doi:10.1016/j.apcatb.2017.01.062.
39. Li Y, Han P, Hou Y, Peng S, Kuang X. Oriented $ZnmIn_2Sm^{+3}$@In_2S_3 Heterojunction with Hierarchical Structure for Efficient Photocatalytic Hydrogen Evolution. *Appl. Catal. B Environ.* **2019**, *244*, 604–611. doi:10.1016/j.apcatb.2018.11.088.
40. Li Y, Li S, Meng L, Peng S. Synthesis of Oriented J Type $ZnIn_2S_4$@$CdIn_2S_4$ Heterojunction by Controllable Cation Exchange for Enhancing Photocatalytic Hydrogen Evolution. *J. Colloid Interface Sci.* **2023**, *650*, 266–274. doi:10.1016/j.jcis.2023.06.185.
41. Li S, Peng S, Li Y. Constructing an Open-Structured J-Type $ZnIn_2S_4$/$In(OH)_3$ Heterojunction for Photocatalytical Hydrogen Generation. *J. Phys. Chem. Lett.* **2024**, *15*, 5215–5222. doi:10.1021/acs.jpclett.4c00835.
42. Phyu Cho P, Phyu Mon P, Ashok Kumar KV, Kumar M, Ghosal P, Lingaiah N, et al. Visible Light Active Cu^{2+} Doped TiO_2 for Simultaneous Removal of Rhodamine-B and Cr (VI). *Inorg. Chem. Commun.* **2023**, *156*, 111147. doi:10.1016/j.inoche.2023.111147.
43. Putri LK, Ong W-J, Chang WS, Chai S-P. Heteroatom Doped Graphene in Photocatalysis: A Review. *Appl. Surf. Sci.* **2015**, *358*, 2–14. doi:10.1016/j.apsusc.2015.08.177.

44. Wang G, Lv S, Shen Y, Li W, Lin L, Li Z. Advancements in Heterojunction, Cocatalyst, Defect and Morphology Engineering of Semiconductor Oxide Photocatalysts. *J. Mater.* **2024**, *10*, 315–338. doi:10.1016/j.jmat.2023.05.014.
45. Das A, SK N, Nair RG. Influence of Surface Morphology on Photocatalytic Performance of Zinc Oxide: A Review. *Nano-Struct. Nano-Objects* **2019**, *19*, 100353. doi:10.1016/j.nanoso.2019.100353.
46. Kumar M, Ghosh CC, Meena B, Ma T, Subrahmanyam C. Plasmonic Au Nanoparticle Sandwiched $CuBi_2O_4/Sb_2S_3$ Photocathode with Multi-Mediated Electron Transfer for Efficient Solar Water Splitting. *Sustain. Energy Fuels* **2022**, *6*, 3961–3974. doi:10.1039/D2SE00600F.
47. Rayalu SS, Jose D, Mangrulkar PA, Joshi M, Hippargi G, Shrestha K, et al. Photodeposition of AuNPs on Metal Oxides: Study of SPR Effect and Photocatalytic Activity. *Int. J. Hydrogen Energy* **2014**, *39*, 3617–3624. doi:10.1016/j.ijhydene.2013.11.120.
48. Yang J, Wang D, Han H, Li C. Roles of Cocatalysts in Photocatalysis and Photoelectrocatalysis. *Acc. Chem. Res.* **2013**, *46*, 1900–1909. doi:10.1021/ar300227e.
49. Su T, Shao Q, Qin Z, Guo Z, Wu Z. Role of Interfaces in Two-Dimensional Photocatalyst for Water Splitting. *ACS Catal.* **2018**, *8*, 2253–2276. doi:10.1021/acscatal.7b03437.
50. Kumar M, Meena B, Subramanyam P, Suryakala D, Subrahmanyam C. Recent Trends in Photoelectrochemical Water Splitting: The Role of Cocatalysts. *NPG Asia Mater.* **2022**, *14*, 88. doi:10.1038/s41427-022-00436-x.
51. Maeda K, Domen K. Development of Novel Photocatalyst and Cocatalyst Materials for Water Splitting under Visible Light. *Bull. Chem. Soc. Jpn.* **2016**, *89*, 627–648. doi:10.1246/bcsj.20150441.
52. Li Y, Li H, Li Y, Peng S, Hu YH. Fe-B Alloy Coupled with Fe Clusters as an Efficient Cocatalyst for Photocatalytic Hydrogen Evolution. *Chem. Eng. J.* **2018**, *344*, 506–513. doi:10.1016/j.cej.2018.03.117.
53. Li Y, Yang T, Li H, Tong R, Peng S, Han X. Transformation of Fe-B@Fe into Fe-B@Ni for Efficient Photocatalytic Hydrogen Evolution. *J. Colloid Interface Sci.* **2020**, *578*, 273–280. doi:10.1016/j.jcis.2020.05.124.
54. Peng S, Yang Y, Tan J, Gan C, Li Y. *In Situ* Loading of Ni_2P on $Cd_{0.5}Zn_{0.5}S$ with Red Phosphorus for Enhanced Visible Light Photocatalytic H_2 Evolution. *Appl. Surf. Sci.* **2018**, *447*, 822–828. doi:10.1016/j.apsusc.2018.04.050.
55. Chen X, Li Y. Solution-Processed Fabrication of Ni_3S_2-Based Nanoheterostructure on Silicon Heterojunction Photocathode for Boosting Solar Hydrogen Generation. *Small Methods* **2024**, 2401075. doi:10.1002/smtd.202401075.
56. Lin S, Huang H, Ma T, Zhang Y. Photocatalytic Oxygen Evolution from Water Splitting. *Adv. Sci.* **2021**, *8*, 2002458. doi:10.1002/advs.202002458.
57. Frame FA, Townsend TK, Chamousis RL, Sabio EM, Dittrich T, Browning ND, et al. Photocatalytic Water Oxidation with Nonsensitized IrO2 Nanocrystals under Visible and UV Light. *J. Am. Chem. Soc.* **2011**, *133*, 7264–7267. doi:10.1021/ja200144w.
58. Gu Q, Gao Z, Yu S, Xue C. Constructing Ru/TiO_2 Heteronanostructures Toward Enhanced Photocatalytic Water Splitting via a RuO_2/TiO_2 Heterojunction and Ru/TiO_2 Schottky Junction. *Adv. Mater. Interfaces* **2016**, *3*, 1500631. doi:10.1002/admi.201500631.
59. Galińska A, Walendziewski J. Photocatalytic Water Splitting over $Pt-TiO_2$ in the Presence of Sacrificial Reagents. *Energy Fuels* **2005**, *19*, 1143–1147. doi:10.1021/ef0400619.
60. Iwashina K, Kudo A. Rh-Doped $SrTiO_3$ Photocatalyst Electrode Showing Cathodic Photocurrent for Water Splitting under Visible-Light Irradiation. *J. Am. Chem. Soc.* **2011**, *133*, 13272–13275. doi:10.1021/ja2050315.
61. Li W, Chu X, Wang F, Dang Y, Liu X, Ma T, et al. Pd Single-Atom Decorated CdS Nanocatalyst for Highly Efficient Overall Water Splitting under Simulated Solar Light. *Appl. Catal. B Environ.* **2022**, *304*, 121000. doi:10.1016/j.apcatb.2021.121000.
62. Iwase A, Kato H, Kudo A. Nanosized Au Particles as an Efficient Cocatalyst for Photocatalytic Overall Water Splitting. *Catal. Lett.* **2006**, *108*, 7–10. doi:10.1007/s10562-006-0030-1.
63. Gogoi D, Namdeo A, Golder AK, Peela NR. Ag-Doped TiO_2 Photocatalysts with Effective Charge Transfer for Highly Efficient Hydrogen Production through Water Splitting. *Int. J. Hydrogen Energy* **2020**, *45*, 2729–2744. doi:10.1016/j.ijhydene.2019.11.127.
64. Yu J, Qi L, Jaroniec M. Hydrogen Production by Photocatalytic Water Splitting over Pt/TiO_2 Nanosheets with Exposed (001) Facets. *J. Phys. Chem. C* **2010**, *114*, 13118–13125. doi:10.1021/jp104488b.
65. Maeda K, Teramura K, Lu D, Takata T, Saito N, Inoue Y, et al. Photocatalyst Releasing Hydrogen from Water. *Nature* **2006**, *440*, 295. doi:10.1038/440295a.
66. Maeda K, Teramura K, Lu D, Saito N, Inoue Y, Domen K. Noble-Metal/Cr_2O_3 Core/Shell Nanoparticles as a Cocatalyst for Photocatalytic Overall Water Splitting. *Angew. Chemie Int. Ed.* **2006**, *45*, 7806–7809. doi:10.1002/anie.200602473.
67. Zou X, Zhang Y. Noble Metal-Free Hydrogen Evolution Catalysts for Water Splitting. *Chem. Soc. Rev.* **2015**, *44*, 5148–5180. doi:10.1039/C4CS00448E.
68. You J, Xiao M, Wang Z, Wang L. Non-Noble Metal-Based Cocatalysts for Photocatalytic CO_2 Reduction. *J. CO2 Util.* **2022**, *55*, 101817. doi:10.1016/j.jcou.2021.101817.
69. Ran J, Zhang J, Yu J, Jaroniec M, Qiao SZ. Earth-Abundant Cocatalysts for Semiconductor-Based Photocatalytic Water Splitting. *Chem. Soc. Rev.* **2014**, *43*, 7787–7812. doi:10.1039/C3CS60425J.

70. Gupta NM. Factors Affecting the Efficiency of a Water Splitting Photocatalyst: A Perspective. *Renew. Sustain. Energy Rev.* **2017**, *71*, 585–601. doi:10.1016/j.rser.2016.12.086.
71. Hisatomi T, Maeda K, Takanabe K, Kubota J, Domen K. Aspects of the Water Splitting Mechanism on $(Ga_{1-x}Zn_x)(N_{1-x}O_x)$ Photocatalyst Modified with $Rh_{2-y}Cr_yO_3$ Cocatalyst. *J. Phys. Chem. C* **2009**, *113*, 21458–21466. doi:10.1021/jp9079662.
72. Zeng D, Li Y. Precisely Loading Pt on Tb_4O_7/CN Heterojunction for Efficient Photocatalytic Overall Water Splitting: Design and Mechanism. *Appl. Catal. B Environ.* **2024**, *342*, 123393. doi:10.1016/j.apcatb.2023.123393.
73. Zhou X, Chen D, Li T, Chen X, Zhu L. Pd and Carbon Quantum Dots Co-Decorated TiO_2 Nanosheets for Enhanced Photocatalytic H_2 Production and Reaction Mechanism. *Int. J. Hydrogen Energy* **2024**, *53*, 1361–1372. doi:10.1016/j.ijhydene.2023.12.004.
74. Pan Z, Vequizo JJM, Yoshida H, Li J, zheng X, Chu C, et al. Simultaneous Structural and Electronic Engineering on Bi- and Rh-co-doped $SrTiO_3$ for Promoting Photocatalytic Water Splitting. *Angew. Chem.* **2024**. doi:10.1002/ange.202414628.
75. Hirayama D, Kawawaki T, Oguchi S, Ogano M, Kon N, Yasuda T, et al. Ultrafine Rhodium–Chromium Mixed-Oxide Cocatalyst with Facet-Selective Loading for Excellent Photocatalytic Water Splitting. *J. Am. Chem. Soc.* **2024**, *146*, 26808–26818. doi:10.1021/jacs.4c07351.
76. Zhang G, Lan Z-A, Lin L, Lin S, Wang X. Overall Water Splitting by Pt/g-C_3N_4 Photocatalysts without Using Sacrificial Agents. *Chem. Sci.* **2016**, *7*, 3062–3066. doi:10.1039/C5SC04572J.
77. Lin Y, Liu Y, Li Y, Cao Y, Huang J, Wang H, et al. Dual Functional CuO_{1-x} Clusters for Enhanced Photocatalytic Activity and Stability of a Pt Cocatalyst in an Overall Water-Splitting Reaction. *ACS Sustain. Chem. Eng.* **2018**, *6*, 17340–17351. doi:10.1021/acssuschemeng.8b04889.
78. Vasilchenko D, Zhurenok A, Saraev A, Gerasimov E, Cherepanova S, Tkachev S, et al. Highly Efficient Hydrogen Production under Visible Light over G-C_3N_4-Based Photocatalysts with Low Platinum Content. *Chem. Eng. J.* **2022**, *445*, 136721. doi:10.1016/j.cej.2022.136721.
79. Yang H, Guo J, Xia Y, Yan J, Wen L. Schottky-Assisted S-Scheme Heterojunction Photocatalyst CdS/Pt@NU-1000 for Efficient Visible-Light-Driven H_2 Evolution. *J. Mater. Sci. Technol.* **2024**, *195*, 155–164. doi:10.1016/j.jmst.2024.01.051.
80. Alharthi FA, Marghany A El, Abduh NAY, Hasan I. Synthesis of Platinum Decorated Bismuth Vanadate (Pt-$BiVO_4$) Nanocomposite for Photocatalytic Hydrogen Production. *React. Kinet. Mech. Catal.* **2024**, *137*, 423–432. doi:10.1007/s11144-023-02520-x.
81. Du X, Liu Q, Cheng M, Wang R, Hu J, Wei T, et al. Single-Atom Pt Decorated g-C_3N_5 Nanorods as Highly Efficient Photocatalyst for H_2 Evolution and Wastewater Purification. *Int. J. Hydrogen Energy* **2024**, *53*, 353–363. doi:10.1016/j.ijhydene.2023.12.035.
82. Kim JH, Wu S, Zdrazil L, Denisov N, Schmuki P. 2D Metal–Organic Framework Nanosheets Based on Pd-TCPP as Photocatalysts for Highly Improved Hydrogen Evolution. *Angew. Chemie Int. Ed.* **2024**, *63*, e202319255. doi:10.1002/anie.202319255.
83. Jiang J, Zhou Y, Zhang J, Gao K, Pan J, Dong P. Accelerating the Charge Separation from the Schottky Junction Effect of Pd-Loaded Al: $SrTiO_3$ for Highly Efficient Photocatalytic Hydrogen Evolution. *Int. J. Hydrogen Energy* **2024**, *82*, 646–654. doi:10.1016/j.ijhydene.2024.07.441.
84. Hussain E, Idrees M, Jalil M, Abid MZ, Aljohani K, Rafiq K. Unveiling the Potential of Cu–Pd/CdS Catalysts to Supply and Rectify Electron Transfer for H_2 Generation from Water Splitting. *Nanoscale* **2025**, *17*, 3436–3450. doi:10.1039/D4NR03381G.
85. Zhou X, Yu X, Peng L, Luo J, Ning X, Fan X, et al. Pd(II) Coordination Molecule Modified g-C_3N_4 for Boosting Photocatalytic Hydrogen Production. *J. Colloid Interface Sci.* **2024**, *671*, 134–144. doi:10.1016/j.jcis.2024.05.150.
86. Abid MZ, Rafiq K, Rauf A, Althomali RH, Hussain E. Scaling up the Charge Transfer on Pd@$Ti_3C_2T_x$–TiO_2 Catalysts: A Sustainable Approach for H_2 Generation via Water Splitting. *Mater. Adv.* **2024**, *5*, 2238–2252. doi:10.1039/D3MA00710C.
87. Pradhan SK, Bhoi YP, Nayak SK, Bariki R, Panda S, Das NK, et al. Facile Fabrication of Pd/CuS/Fe_2O_3 Ternary Nanocomposite: A Plasmonic Metal Endorsed p-n Heterostructure with Synergistic Charge Migration for Enhanced Photoreduction Reactions. *Mater. Today Chem.* **2024**, *36*, 101947. doi:10.1016/j.mtchem.2024.101947.
88. Huang J, Qiu J, Yang Y, Li B, Wang L, Cheng H-M, et al. Interface Regulation of Bi_3TiNbO_9/Rh Photocatalysts by Introducing Ultrathin Heterolayer to Enhance Overall Water Splitting. *Adv. Funct. Mater.* **2024**, *34*, 2402711. doi:10.1002/adfm.202402711.
89. Vennapoosa CS, Karmakar A, Prabhu YT, Abraham BM, Kundu S, Pal U. Rh-Doped Ultrathin NiFeLDH Nanosheets Drive Efficient Photocatalytic Water Splitting. *Int. J. Hydrogen Energy* **2024**, *52*, 371–384. doi:10.1016/j.ijhydene.2023.02.025.
90. Jing H, Li H, Yue J, Fan S, Yao B, Liu S, et al. Synergistic Effects of the Rh–S Bond and Spatially Separated Dual Cocatalysts on Photocatalytic Overall Water Splitting Activity of $ZnIn_2S_4$ Nanosheets under Visible Light Irradiation. *Dalt. Trans.* **2023**, *52*, 2924–2927. doi:10.1039/D3DT00050H.
91. Li Z, Li R, Jing H, Xiao J, Xie H, Hong F, et al. Blocking the Reverse Reactions of Overall Water Splitting on a Rh/GaN–ZnO Photocatalyst Modified with Al_2O_3. *Nat. Catal.* **2023**, *6*, 80–88. doi:10.1038/s41929-022-00907-y.
92. Thabet SM, Abdelhamid HN, Ibrahim SA, El-Bery HM. Boosting Photocatalytic Water Splitting of TiO_2 Using Metal (Ru,

Co, or Ni) Co-Catalysts for Hydrogen Generation. *Sci. Rep.* **2024**, *14*, 10115. doi:10.1038/s41598-024-59608-0.
93. Liu Y, Miao J, Zhang W, Wei A, Wang J. *In-Situ* Photodeposition of Co-Catalyst Ni_2P on CdS for Photocatalytic Conversion of Ethanol for Synergistic Hydrogen Production. *J. Fuel Chem. Technol.* **2024**, *52*, 1629–1640. doi:10.1016/S1872-5813(24)60493-7.
94. Song J, Su H-Y, Zhong G, Liu Y, Huang X, Zhou J, et al. Photosynthesis Assembling of ZCS/PO/Ni_3Pi_2 Catalyst for Three-Stage Photocatalytic Water Splitting into H_2 and H_2O_2. *Colloids Surf. A Physicochem. Eng. Asp.* **2023**, *656*, 130417. doi:10.1016/j.colsurfa.2022.130417.
95. Cao X, Xing S, Ma D, Tan Y, Zhu Y, Hu J, et al. Design of High-Performance Ion-Doped CoP Systems for Hydrogen Evolution: From Multi-Level Screening Calculations to Experiment. *J. Energy Chem.* **2023**, *82*, 307–316. doi:10.1016/j.jechem.2023.03.043.
96. Zhao H, Yang L, Zhang Z, Hei Y, Li W, Lu Z, et al. The Visible-Light-Driven Photocatalytic Performance in H_2 Evolution for Core-Shell CN@CoP Heterojunction. *Ceram. Int.* **2023**, *49*, 1230–1237. doi:10.1016/j.ceramint.2022.09.101.
97. Zhao F, Yang X, Xiong S, Li J, Fu H, An X. Efficient Schottky Heterojunctions of CoP Nanoparticles Decorated Mn-Doped CdS Nanorods for Photocatalytic Hydrogen Evolution by Water Splitting. *Int. J. Hydrogen Energy* **2024**, *89*, 434–442. doi:10.1016/j.ijhydene.2024.09.334.
98. Hinnemann B, Moses PG, Bonde J, Jørgensen KP, Nielsen JH, Horch S, et al. Biomimetic Hydrogen Evolution: MoS_2 Nanoparticles as Catalyst for Hydrogen Evolution. *J. Am. Chem. Soc.* **2005**, *127*, 5308–5309. doi:10.1021/ja0504690.
99. Wei X, Wang M, Ali S, Wang J, Zhou Y, Zuo R, et al. Enhanced Photocatalytic H_2 Evolution on G-C_3N_4 Nanosheets Loaded with Nitrogen-Doped MoS_2 as Cocatalysts. *Int. J. Hydrogen Energy* **2024**, *89*, 691–702. doi:10.1016/j.apsusc.2018.07.154.
100. Wang Y, Pajares A, Serafin J, Alcobé X, Güell F, Homs N, et al. MoxC Heterostructures as Efficient Cocatalysts in Robust MoxC/g-C_3N_4 Nanocomposites for Photocatalytic H_2 Production from Ethanol. *ACS Sustain. Chem. Eng.* **2024**, *12*, 4365–4374. doi:10.1021/acssuschemeng.3c06261.
101. Wang J, Tian J, Han P, Song L, Wang W, Lin K, et al. Enhanced Photocatalytic Hydrogen Production Activity Driven by TiO_2/(MoP/CdS): Insights from Powder Particles to Thin Films. *Langmuir* **2024**, *40*, 21161–21170. doi:10.1021/acs.langmuir.4c02635.
102. Talebi P, Kistanov AA, Rani E, Singh H, Pankratov V, Pankratova V, et al. Unveiling the Role of Carbonate in Nickel-Based Plasmonic Core@shell Hybrid Nanostructure for Photocatalytic Water Splitting. *Appl. Energy* **2022**, *322*, 119461. doi:10.1016/j.apenergy.2022.119461.
103. Saleem F, Abid MZ, Rafiq K, Rauf A, Ahmad K, Iqbal S, et al. Synergistic Effect of Cu/Ni Cocatalysts on CdS for Sun-Light Driven Hydrogen Generation from Water Splitting. *Int. J. Hydrogen Energy* **2024**, *52*, 305–319. doi:10.1016/j.ijhydene.2023.05.048.
104. Li S, Li Y, Yin W, Su K, He P, Chen J, et al. Boosting the Photocatalytic Hydrogen Production Activity of Marigold-like $Zn_2In_2S_5$ by Using Noble-Metal-Free Ni_2P as Cocatalyst. *Int. J. Hydrogen Energy* **2024**, *56*, 596–603. doi:10.1016/j.ijhydene.2023.12.267.
105. Lu Y, Liu J, Hu B, Yang H, Chen Y, Xie Y, et al. Ni_2P Co-Catalyst Modification CdS Enhancement Hydrogen Evolution and Keeping Strong Stability under Visible Light. *Sep. Purif. Technol.* **2025**, *360*, 131104. doi:10.1016/j.seppur.2024.131104.
106. Chen W, Wang Y, Liu M, Gao L, Mao L, Fan Z, et al. *In Situ* Photodeposition of Cobalt on CdS Nanorod for Promoting Photocatalytic Hydrogen Production under Visible Light Irradiation. *Appl. Surf. Sci.* **2018**, *444*, 485–490. doi:10.1016/j.apsusc.2018.03.068.
107. Zhao N, Kong L, Dong Y, Wang G, Wu X, Jiang P. Insight into the Crucial Factors for Photochemical Deposition of Cobalt Cocatalysts on G-C_3N_4 Photocatalysts. *ACS Appl. Mater. Interfaces* **2018**, *10*, 9522–9531. doi:10.1021/acsami.8b01590.
108. Chen F, Jiao P, Zhao C. Single-Atom Cobalt Decorated P-Doped g-C_3N_4 for Efficient Visible-Light-Driven Water Splitting. *Catal. Lett.* **2024**, *154*, 2579–2589. doi:10.1007/s10562-023-04494-w.
109. Zhang X, Wu F, Li G, Wang L, Huang J, Song A, et al. Dual Electric Field Coupling with Tunable Schottky Barrier Synergistically Regulating Electronic Configuration in CoP@Ni-CdS Heterojunction for Efficient Photocatalytic H_2 Evolution. *Adv. Funct. Mater.* **2025**, *35*, 2412527. doi:10.1002/adfm.202412527.
110. Li S, Ye J, Fan Z, Dai Y, Xie Y, Ling Y, et al. CoP Co-Catalyst Modification $ZnIn_2S_4$ Driving Efficient H_2 Evolution under Visible Light. *Sep. Purif. Technol.* **2025**, *358*, 130294. doi:10.1016/j.seppur.2024.130294.
111. Zhang S, Li S, Zhou M, Li X, Wang Y, Suo S, et al. Modulating Long-Lived Ultrafast Charge Carrier Recombination in Type-I MoS_2/CdS Photocatalyst Achieving Optimal H_2 Evolution. *Sep. Purif. Technol.* **2025**, *355*, 129664. doi:10.1016/j.seppur.2024.129664.
112. Muthukumar R, Balaji G. Noble Metal-Free Ternary MoS_2/g-C_3N_4/$ZnIn_2S_4$ Heterojunction with Efficient Charge Transfer for Highly Efficient Photocatalytic H_2 Production. *Diam. Relat. Mater.* **2025**, *152*, 111941. doi:10.1016/j.diamond.2024.111941.
113. Liu Y, Yang Z, Ng YH, Chen J, Li J, Gan Q, et al. Interplay between the Interfacial Mo–N Bonds within MoC Nanodot/N-Doped Carbon Composites for Efficient Photocatalytic Reduction of Cr(VI) and Hydrogen Evolution Reaction. *J. Mater. Sci. Technol.* **2025**, *215*, 147–156. doi:10.1016/j.jmst.2024.05.073.
114. Li X-A, Tan L-L, Wang X-L, Liu Y, Liang Z-Z, Huang J-F, et al. A Z-Scheme Photosensitive MOC/g-C_3N_4 Composite

Catalyst for Efficient Visible-Light Driven Half and Overall Water Splitting. *J. Mater. Chem. A* **2024**, *12*, 32307–32317. doi:10.1039/D4TA06849A.

115. Wang W, Zhang Y, Chang H, Hu S, Qiu R, Zhang M, et al. Revolutionary Amorphous MoP Quantum Dots as Efficient Visible Light Harvester Coupled with SiC for Boosting Photocatalytic Hydrogen Production. *Renew. Energy* **2024**, *235*, 121389. doi:10.1016/j.renene.2024.121389.
116. Bian Z, Feng S, Wang H, Ma C, Dai X, Wu K, et al. Ohmic Junction $ZnIn_2S_4$/MoP for Efficient Photocatalytic Hydrogen Evolution. *Phys. B Condens. Matter* **2024**, *688*, 415886. doi:10.1016/j.physb.2024.415886.
117. Sindhu M, Sharma A, Maan KS, Patel V, Singh PP, Nguyen V-H. Fabrication and Characterization of Novel V, S Co-Doped Ta_3N_5 Protected with PANI Composite Materials for Hydrogen Generation from Light-Driven Water Splitting. *J. Taiwan Inst. Chem. Eng.* **2024**, *158*, 105024. doi:10.1016/j.jtice.2023.105024.
118. Ghosh S, Kouamé NA, Ramos L, Remita S, Dazzi A, Deniset-Besseau A, et al. Conducting Polymer Nanostructures for Photocatalysis under Visible Light. *Nat. Mater.* **2015**, *14*, 505–511. doi:10.1038/nmat4220.
119. Ghosh S, Bera S, Sardar S, Pal S, Camargo FVA, D'Andrea C, et al. Role of Efficient Charge Transfer at the Interface between Mixed-Phase Copper-Cuprous Oxide and Conducting Polymer Nanostructures for Photocatalytic Water Splitting. *ACS Appl. Mater. Interfaces* **2023**, *15*, 18867–18877. doi:10.1021/acsami.3c00090.
120. Wang J, Han F, Rao Y, Hu T, Huang Y, Cao J, et al. Visible-Light-Driven Nitrogen-Doped Carbon Quantum Dots/$CaTiO_3$ Composite Catalyst with Enhanced NO Adsorption for NO Removal. *Ind. Eng. Chem. Res.* **2018**, *57*, 10226–10233. doi:10.1021/acs.iecr.8b01731.
121. Raghavan A, Sarkar S, Nagappagari LR, Bojja S, MuthukondaVenkatakrishnan S, Ghosh S. Decoration of Graphene Quantum Dots on TiO_2 Nanostructures: Photosensitizer and Cocatalyst Role for Enhanced Hydrogen Generation. *Ind. Eng. Chem. Res.* **2020**, *59*, 13060–13068. doi:10.1021/acs.iecr.0c01663.
122. Sindhu M, Sharma A, Maan KS, Patel V, Singh PP, Nguyen B-S, et al. Nb-Ta_3N_5 Protected with PANI Nanocomposite for Enhanced Photocatalytic Water-Splitting towards Hydrogen Production under Visible Light Irradiation. *Mater. Lett.* **2024**, *359*, 135895. doi:10.1016/j.matlet.2024.135895.
123. Sindhu M, Sharma A, Patel V, Gahlawat A, Singh PP, Maan KS, et al. Characteristic Studies of Ta_3N_5/BSC@PANI Nanocomposites for Hydrogen Production via Water-Splitting under Visible Light Irradiation. *Chem. Eng. Res. Des.* **2023**, *197*, 572–580. doi:10.1016/j.cherd.2023.07.050.
124. Hait P, Mehta R, Basu S. Advancing Sustainable Solutions: Harnessing Polyaniline/BiOCl/GO Ternary Nanocomposites for Solar-Powered Degradation of Organic Pollutant and Photocatalytic Hydrogen Generation. *J. Clean. Prod.* **2023**, *424*, 138851. doi:10.1016/j.jclepro.2023.138851.
125. Dustgeer MR, Jilani A, Ansari MO, Shakoor MB, Ali S, Imtiaz A, et al. Reduced Graphene Oxide Supported Polyaniline/Copper (II) Oxide Nanostructures for Enhanced Photocatalytic Degradation of Congo Red and Hydrogen Production from Water. *J. Water Process Eng.* **2024**, *59*, 105053. doi:10.1016/j.jwpe.2024.105053.
126. Wei P, Zhang P, Zhang Y, Li X. Highly Efficient Photocatalytic Overall Water Splitting on Plasmonic Cu_6Sn_5/Polyaniline Nanocomposites. *J. Colloid Interface Sci.* **2022**, *609*, 785–793. doi:10.1016/j.jcis.2021.11.090.
127. Han Z, Dong Q, Chen G, Dong H, Zhou R. Interface Cd-N Bond Bridge Accelerating Charge Separation to the Enhanced Visible Light Driven Hydrogen Production from Water Splitting on Polyaniline@Cd-Zn-S Photocatalyst. *Sep. Purif. Technol.* **2022**, *300*, 121839. doi:10.1016/j.seppur.2022.121839.
128. Ghosh S, Pal S, Biswas M, Thandavarayan M, Reddy AA, Naskar MK. Dual Active Site Mediated Photocatalytic H_2 Evolution through Water Splitting Using CeO_2/PPy/BFO Double Heterojunction Catalyst. *ACS Appl. Energy Mater.* **2024**, *7*, 11453–11465. doi:10.1021/acsaem.4c00269.
129. Pal S, Das PS, Naskar MK, Ghosh S. Metal Oxide Nanocrystals Embedded Polypyrrole Nanohybrid: Exploring Role of Interface in Photocatalytic Hydrogen Generation. *Mater. Today Sustain.* **2024**, *25*, 100610. doi:10.1016/j.mtsust.2023.100610.
130. Xue J, Zhang H, Shen Q, Zhang W, Gao J, Li Q, et al. Enhanced Photoelectrocatalytic Hydrogen Production Performance of Porous MoS_2/PPy/ZnO Film under Visible Light Irradiation. *Int. J. Hydrogen Energy* **2021**, *46*, 35219–35229. doi:10.1016/j.ijhydene.2021.08.083.
131. Kumar Das K, Sahoo DP, Mansingh S, Parida K. $ZnFe_2O_4$@WO_{3-X}/Polypyrrole: An Efficient Ternary Photocatalytic System for Energy and Environmental Application. *ACS Omega* **2021**, *6*, 30401–30418. doi:10.1021/acsomega.1c03705.
132. Peng X, Li J, Yi L, Liu X, Chen J, Cai P, et al. Ultrathin $ZnIn_2S_4$ Nanosheets Decorating PPy Nanotubes toward Simultaneous Photocatalytic H_2 Production and 1,4-Benzenedimethanol Valorization. *Appl. Catal. B Environ.* **2022**, *300*, 120737. doi:10.1016/j.apcatb.2021.120737.
133. Wang J, Liu R, Qiao Y, Liu S, Qin C. Graphene Quantum Dot @ Flower-like Bi_2S_3 Composites for Photodegradation of Organic Pollutants Combined Photosynthesis of H_2 and H_2O_2 from Treated Water. *Int. J. Hydrogen Energy* **2025**, *98*, 1464–1477. doi:10.1016/j.ijhydene.2024.12.126.
134. Backes CW, Reis FB, Strapasson GB, Assis M, Longo E, Weibel DE. Green Synthesis of Carbon Quantum Dots for Enhancing Photocatalytic Activity: Hydrogen/Oxygen Evolution and Dye Photodegradation. *Catal. Today* **2025**, *443*, 114996. doi:10.1016/j.cattod.2024.114996.

135. Fu M, Yu S, Zhong Y, Chen Y, Duan C, Guo H, et al. S and N Codoped Graphene Quantum Dots Decorated on (001) TiO_2 to Boost Surface Reaction for Photocatalytic Hydrogen Production. *Results Surf. Interfaces* **2024**, *14*, 100181. doi:10.1016/j.rsurfi.2024.100181.
136. Li N, Ma J, Wang W, Chang Q, Liu L, Hao C, et al. Dual S-Scheme MoS_2/$ZnIn_2S_4$/Graphene Quantum Dots Ternary Heterojunctions for Highly Efficient Photocatalytic Hydrogen Evolution. *J. Colloid Interface Sci.* **2024**, *676*, 496–505. doi:10.1016/j.jcis.2024.07.144.
137. Zou J-P, Wang L-C, Luo J, Nie Y-C, Xing Q-J, Luo X-B, et al. Synthesis and Efficient Visible Light Photocatalytic H_2 Evolution of a Metal-Free g-C_3N_4/Graphene Quantum Dots Hybrid Photocatalyst. *Appl. Catal. B Environ.* **2016**, *193*, 103–109. doi:10.1016/j.apcatb.2016.04.017.
138. Min S, Hou J, Lei Y, Ma X, Lu G. Facile One-Step Hydrothermal Synthesis toward Strongly Coupled TiO_2/Graphene Quantum Dots Photocatalysts for Efficient Hydrogen Evolution. *Appl. Surf. Sci.* **2017**, *396*, 1375–1382. doi:10.1016/j.apsusc.2016.11.169.